Report 555034003

Relationship between aerosol optical depth and $PM_{2.5}$ in the Netherlands

SATLINK final report

Netherlands Environmental Assessment Agency

TNO

rivm

Relationship between aerosol optical depth and $PM_{2.5}$ in the Netherlands

SATLINK final report

Report 555034003

Relationship between aerosol optical depth and $PM_{2.5}$ in the Netherlands

SATLINK final report

This investigation was co-funded by the Netherlands Agency for Aerospace Programmes (NIVR), within the framework of the project SATLINK, NIVR project code 53.614RI.
PBL, P.O. Box 303, 3720 AH Bilthoven, telephone: 31 - 30 274 2745; www.pbl.nl

MNP en RPB vormen sinds april 2008 het Planbureau voor de Leefomgeving

Relationship between aerosol optical depth and $PM_{2.5}$ in the Netherlands
SATLINK final report

PBL-publicationnumber 555034003

M. Schaap*
A. Apituley#
R.B.A. Koelemeijer@
R.M.A. Timmermans*
R. Schoemaker+
J. Matthijsen@
G. de Leeuw*

* TNO Bouw en Ondergrond
# Rijksinstituut voor Volksgezondheid en Milieu
@ Planbureau voor de Leefomgeving
+ TNO Defensie en Veiligheid

Contact
Robert Koelemeijer
Robert.Koelemeijer@mnp.nl
030-2743289

Netherlands Environmental Assessment Agency

PO Box 303
3720 AH Bilthoven
Phone: +31 (0) 30 274 274 5
Fax: +31 (0) 30 274 44 79
E-mail: info@pbl.nl
Website: www.pbl.nl

Rapport in het kort

Dit rapport beschrijft een verkennende studie naar het gebruik van satellietgegevens voor het bestuderen van de fijnere fractie van fijn stof ($PM_{2.5}$). Satellietinstrumenten meten niet direct $PM_{2.5}$, maar meten de z.g. Aerosol Optische Dikte (AOD), wat een optische maat is voor de hoeveelheid stof in de gehele atmosferische kolom boven een deel van het aardoppervlak. De relatie tussen AOD en $PM_{2.5}$ is onderzocht op de meetlocatie Cabauw in de periode 2006 - 2007. In maanden met weinig bewolking correleren de AOD en $PM_{2.5}$ metingen behoorlijk goed, met een lineaire correlatie van typisch R^2=0.6. Satellietmetingen van de AOD zouden dus gebruikt kunnen worden als proxy voor variaties in de tijd van de $PM_{2.5}$ concentratie.

De gemeten $PM_{2.5}$ concentratie in Cabauw gemiddeld over de periode augustus 2006 tot mei 2007 is 18 $\mu g/m^3$, wat illustreert dat Nederland een hoge achtergrondconcentratie heeft in vergelijking tot veel andere gebieden in Europa. De tijdscorrelatie tussen AOD en $PM_{2.5}$ is vooral goed in situaties met overheersend oostelijke en zuidelijke windrichtingen. De gevonden lineaire relatie tussen AOD en $PM_{2.5}$ is toegepast op satellietmetingen van MODIS om een kaart te maken van $PM_{2.5}$ in Nederland en omgeving. De interpretatie van deze kaart behoeft nadere aandacht omdat de ruimtelijke variaties van de AOD over Nederland van vergelijkbare omvang zijn als de foutenmarge in de AOD metingen. Dit laatste leidt tot duidelijke artefacten in de verdeling. Daarnaast is de kaart afgeleid voor dagen met (zuid-) oostelijke stroming over Nederland en beschrijft deze de situatie rond het middaguur. Aanvullende modelberekeningen en een evaluatie met metingen zijn nodig om te onderzoeken hoe de verdeling zich verhoudt ten opzichte van andere meteorologische situaties. Door intrinsieke beperkingen van satelliet gegevens van fijn stof is het niet te verwachten dat in de nabije toekomst betere $PM_{2.5}$ kaarten kunnen worden gemaakt op basis van de gegevens alleen. De toegevoegde waarde van satelliet gegevens van fijn stof zal vooral tot uitdrukking komen wanneer ze gecombineerd worden met modelberekeningen en metingen van fijn stof op leefniveau.

Contents

Executive summary *9*

1 Introduction *11*

2 Experimental set-up *15*
- 2.1 Ground-based data sources *15*
- 2.2 Satellite data sources *19*
- 2.3 Data processing *23*
- 2.4 Analysis procedure *24*

3 Overview of ground-based data *25*
- 3.1 Statistics *25*
- 3.2 Initial comparison between AOD and $PM_{2.5}$ *25*
- 3.3 Examples of vertical aerosol profiles *28*

4 Analysis of AERONET AOD data *31*
- 4.1 Cloud detection methods *31*
- 4.2 Evaluation of cloud indicators *34*
- 4.3 Impact of AERONET v1.5 data *35*

5 Analysis of the relationship between AOD and $PM_{2.5}$ *39*
- 5.1 Correlation between filtered AOD and $PM_{2.5}$ *39*
- 5.3 Sensitivity to the time of the day *41*
- 5.4 Influence of air mass origin *42*
- 5.5 Relationship between AOD and $PM_{2.5}$ at Cabauw - synthesis *44*
- 5.6 Discussion *44*

6 $PM_{2.5}$ estimation from satellite AOD *49*
- 6.1 Satellite derived AOD fields *49*
- 6.2 Satellite data evaluation *49*
- 6.3 Satellite AOD versus ground level $PM_{2.5}$ *52*
- 6.4 Satellite derived $PM_{2.5}$ maps *52*
- 6.5 Discussion *55*
- 6.6 Cost benefit analysis *56*

7 Summary and conclusions *57*

Acknowledgements *59*
References *61*

Appendix A: Outreach *63*
Appendix B: Effect of cloud screening for Spring 2007 *65*
Appendix C: National User Support Programme 2001-2005 *67*

Executive summary

Health effects of air pollution in Europe are dominated by particulate matter. New air quality standards for $PM_{2.5}$ have been set in the new EU air quality directive. However, uncertainties in $PM_{2.5}$ distributions are still large, and efforts to monitor and model $PM_{2.5}$ need to be intensified to improve this. Many studies in the last few years have shown the potential of satellite measurements to aid monitoring $PM_{2.5}$ concentrations at surface level.

An explorative study was carried out to investigate the use of satellite observations to monitor temporal and spatial variations in particulate matter ($PM_{2.5}$) in the Netherlands. To this end, a data set on AOD and $PM_{2.5}$ at the atmospheric monitoring site, Cabauw, in a rural area in the centre of the Netherlands. Since August 2006, $PM_{2.5}$ has been monitored at Cabauw as well as other atmospheric parameters including (AOD) using a Cimel sun photometer, and LIDAR backscatter profiles. An analysis of measurements at Cabauw is presented directed to quantification of the relationship between AOD and $PM_{2.5}$ in the first year of observations. This relationship was studied using ground-based (AERONET) as well as satellite based (MODIS and AATSR) measurements of AOD.

The AERONET L1.5 data on AOD used in this study has revealed a relatively large number of high AOD values paired to low $PM_{2.5}$ values, suggesting cloud contamination. Various methods were used to detect cloud contamination in the AERONET data in order to substantiate this hypothesis. A cloud screening method based on LIDAR observations was chosen to detect clouds in the AERONET L1.5 data. Application of this method led to rejection of about 50% of the AERONET L1.5 data because of suspected cloud contamination. Comparison with AERONET L2.0 data that were available towards the end of the project shows that almost half of the AERONET L1.5 data was not maintained in the L2.0 data set, and that the L2.0 data set was almost identical to the cloud-screened L1.5 data set as used in this study. This gives confidence in both our cloud-screening method and in the cloud-screening method used by AERONET to process L1.5 to L2.0.

Subsequently, the dependence of the relationship between AOD and $PM_{2.5}$ was studied as a function of the time of day, boundary layer height and air mass origin. The temporal correlation between AOD and $PM_{2.5}$ was found to increase when only data were used that had been obtained around noon. This time coincides with the time of overpass of the MODIS and AATSR satellites. Several factors may explain the increase in the explained variability when the data are confined to around mid-day. During conditions with valid AOD retrievals the mixing layer height during midday is generally well mixed, without residual layers present. Another important factor may be related to the solar zenith angle because a sun photometer is pointed directly at the sun. AOD measurements under large solar-zenith angles (low sun) are associated with much higher relative air-mass factors compared to mid-day. This means that the relative contribution of aerosols in atmospheric layers above the mixing layer may become more important at large solar zenith angles. Furthermore, an averaging effect occurs in the observed aerosol properties and correlation with local observations decreases. Therefore, variability in observed AOD is expected to be higher under small solar-zenith angles. Finally, cloud screening using the LIDAR is probably more accurate during midday as the LIDAR profiles the atmosphere directly above the site. Under large solar zenith angles, the observed part of the sky will be rather different between sun photometer and LIDAR. Better similarity is obtained under small solar zenith angles. Contra intuitively, the AOD-$PM_{2.5}$ correlation did not improve after accounting for variation in the mixing layer height. This contrasts with other studies that show a strong dependence of the AOD-PM

relationship on mixing layer height and relative humidity (e.g., Gupta, 2006; Koelemeijer et al., 2006a, b). This may be due to the fact that the mixing layer did not show a strong seasonal cycle over the Cabauw site during the year, unlike many other stations in Europe that were studied in earlier work. AOD data can only be obtained during clear sky conditions, and is biased towards conditions of southerly and easterly wind directions. Under such conditions, the temporal variations of AOD was shown to correlate reasonably well with temporal variations in $PM_{2.5}$ (R^2=0.6). This suggests that temporal variations of satellite AOD can be used as a proxy for temporal variations in $PM_{2.5}$. For these conditions, and limiting the data set to observations around noon, the following AOD-$PM_{2.5}$ relationship was found for Cabauw: $PM_{2.5}$ =F 124.5*AOD – 0.34. The difference between the yearly average $PM_{2.5}$ data (obtained for all conditions) and the $PM_{2.5}$ data for conditions with predominantly southerly and easterly flow is typically 45%.

The average $PM_{2.5}$ concentration at Cabauw of 18 μg/m³ is high in comparison with rural areas in Europe and confirms that the Netherlands are characterised by a high PM burden. Satellite-derived AOD maps from AATSR and MODIS show similar mean values, but observed features in the spatial distributions are distinctly different. This illustrates that the interpretation of the AOD maps in terms of PM is hampered because the systematic errors in AOD of the same order of magnitude as the spatial variations themselves.

There was no opportunity to validate the spatial distribution of $PM_{2.5}$ derived from MODIS AOD measurements because of lack of well-calibrated $PM_{2.5}$ ground-based measurements in the period concerned. Thus, the estimated $PM_{2.5}$ distribution is preliminary and the validity and utility of the proposed mapping methodology should be further investigated. For this purpose, a number of sites with identical PM monitoring equipment further away from the coast should be used. Validation of the $PM_{2.5}$ fields is also hampered because different atmospheric transport models show different spatial structures over the Netherlands, stemming from uncertainties about emissions as well as different treatment of atmospheric chemistry. Moreover, comparisons with modelled yearly average fields are difficult to make as the $PM_{2.5}$ field presented holds for conditions with southerly and easterly flows over the Netherlands and is representative for the daytime. Nevertheless, some features of the spatial distribution within the Netherlands do not appear to be realistic. Such artefacts might be caused by systematic errors present in the MODIS AOD data, particularly over coastal areas and areas with inland surface water such rivers and lakes.

An earlier project (PARMA) has shown that at larger scales (Europe), the spatial distribution of AOD has more realistic structures. The reason may be that over the whole of Europe, spatial gradients in AOD are larger than within the Netherlands, while many parts of continental Europe are much less affected by the presence of mixed land/water pixels than is the case within the Netherlands. Because of the uncertainties in current satellite data of AOD, it is not expected that improved $PM_{2.5}$ maps can be constructed based on satellite data only in the near future. Satellite measurements of AOD will have added-value particularly regarding the temporal variation of PM, when they are combined with atmospheric transport models and surface measurements of $PM_{2.5}$.

1 Introduction

While air quality in Europe has improved substantially over the last few decades, air pollution still poses a significant threat to human health (EEA, 2007). Health effects of air pollution are dominated by particulate matter, both $PM_{2.5}$ (particles of 2.5 µm diameter or less), and PM_{10} (particles of 10 µm diameter or less). Short-term exposure to particulate matter has frequently been associated with increased human morbidity and mortality (e.g., Dockery et al., 1993; Brunekreef and Holgate, 2002).

While less is known about the effects of long-term exposure than of short-term exposure to particulate matter the health impacts are thought to be much greater (Pope III et al., 1995). An analysis by the World Health Organization (WHO, 2006) indicates that air polluted with particulate matter, and especially fine fraction ($PM_{2.5}$), affects the health of most of Europe's population. This leads to a wide range of acute and chronic health problems, and reduces life expectancy by almost one year on average in the EU Member States (WHO, 2006).

To prevent these negative health effects, the EU has set two limit values for PM_{10}:
- and a limit value of 40 µg/m³ for the a limit value for 24-hour average concentrations, of 50 µg/m³ that may not be exceeded more than 35 times per year;
- annual average concentration.

Recently, political agreement was reached to establish new limit values for $PM_{2.5}$:
- a limit value of 25 µg/m³ for the annual average concentration, to be attained by 2015 that is applicable everywhere;
- a so-called exposure concentration obligation of 20 µg/m³ to be attained in 2015, which holds for the average urban background concentration;

In addition, other goals were set that are not yet juridically binding. The urban background concentration of $PM_{2.5}$ should be decreased by 0 to 20% between 2010 and 2020, based on the concentration level in 2010. The target of 20% is for the most polluted urban areas, while there is no obligation to reduce the concentration in urban areas with yearly average $PM_{2.5}$ concentrations below 7 µg/m³. Also, an indicative limit value of 20 µg/m³ is established for annual average PM2.5 concentrations, to be attained in 2020.

Air quality measurements

To monitor compliance with the limit values, air quality is measured in all EU Member States. The data are stored in a central database, Airbase, which is maintained by the European Environment Agency.

Although these ground-based measurements are relatively accurate, they are representative of a limited area because aerosol sources vary over small spatial scales and the aerosol lifetime is less than an hour to a few days, depending on particle size and chemical composition.

Furthermore, the difficulty of measuring the absolute level of PM is widely recognised. The measurement error is estimated to be 20% for yearly average concentrations (1-sigma). One of the problems with PM measurement is the volatilisation of the semi-volatile components during the measurement process. This leads to systematic measurement errors depending on the measurement technique used and aerosol composition which varies in time. These systematic errors are corrected with a fixed correction factor in some EU Member States but no correction is

made in some other countries. The limited spatial representativeness and systematic errors make it virtually impossible to achieve an accurate overview across Europe based on ground-based measurements only.

Satellite measurements

Satellite measurements are less precise but provide a large spatial coverage and have the advantage of being country-independent. Thus, satellite measurements could be used to complement the surface network to achieve greater comparability of PM levels between countries.

Since 2000, the usefulness of satellite measurements of Aerosol Optical Depth (AOD) to improve $PM_{2.5}$ monitoring has been investigated in a rapidly increasing number of studies. Several studies in the USA have reported good temporal correlations between satellite derived AOD and $PM_{2.5}$ surface concentration measurements. (Wang and Christopher, 2003; Hutchison, 2003). In general, promising correlations have been found between one-month time-series of AOD and $PM_{2.5}$ for many stations in the Eastern and Midwest of the USA. Other stations, however, particularly in the west of the country show hardly any correlation (Engel-Cox et al., 2004; 2006). The strength of such correlations is likely to be affected by factors such as variations in local meteorological conditions, occurrence of multiple aerosol layers, and variations in aerosol chemical composition.

Van Donkelaar et al. (2006) studied the usefulness of satellite AOD measurements of the Moderate Resolution Imaging Spectroradiometer (MODIS) and the Multi-angle Imaging Spectroradiometer (MISR) for assessment of spatial variations of $PM_{2.5}$ in North America. They concluded that there is significant agreement with those from the surface networks in Canada (NAPS) and the USA (AQS).

Recent studies in other regions including Europe have indicated the use of satellite measurements in monitoring particulate matter air quality (Chu et al., 2003; Koelemeijer et al., 2006a; Kacenelenbogen, et al., 2006; Gupta et al., 2006; Gupta et al., 2007). Several studies have also showed that the relationship between PM and AOD is influenced by the mixing layer height and relative humidity (e.g., Gupta, 2006; Koelemeijer et al., 2006a, b). The studies above have concluded that AOD observations may be useful in improving mapping of PM concentrations.

A PM10 distribution for Europe has been derived using geo-statistical techniques combining in-situ observations, modelled distributions and MODIS (MODerate-resolution Imaging Spectroradiometer) satellite data (van de Kassteele et al., 2006; NIVR PARMA project). Use of both model and remote sensing data have been shown to improve the quality of the estimated annual average PM10 distribution. A more direct estimate of global PM2.5 was made using modelled AOD-PM2.5 relationships to satellite-derived AOD (van Donckelaar et al., 2006). Furthermore, the advent of satellite observations has led to a development of data assimilation schemes that assimilate AOD directly into models (e.g., Builtjes et al., 2001; Collins et al., 2001; Koelemeijer et al., 2006a). In the latter approaches, used in NIVR PARMA and HIRAM projects, the modelled relation between AOD and PM2.5 is a very uncertain and limiting factor in determining the absolute PM2.5 concentrations from satellite data (Koelemeijer et al., 2006a).

Study objectives

In acquiring daily estimates of $PM_{2.5}$ distributions, the critical factors are the quality of the remote sensing data and an established relationship between AOD and ground-level $PM_{2.5}$. In this study, we aimed to establish experimentally this relationship for the Netherlands. For this

purpose, a field study was conducted at Cabauw, the central site for atmospheric research in the Netherlands. Furthermore, we aim to demonstrate the feasibility of using the relationship to map $PM_{2.5}$ over the Netherlands using satellite data.

This study is co-funded by the Netherlands Agency for Aerospace Programmes (NIVR) under the National User Support Programme (see Appendix C). It builds on experience obtained in a series of previous NIVR projects: ARIA2, PARMA and HIRAM.

2 Experimental set-up

2.1 Ground-based data sources

In this study, ground-based measurements of aerosol optical depth (AOD) were related to ground-based measurements of particulate matter. For this study, the co-location of ground-based data sources is critical, since atmospheric variability and spatial inhomogeneity rapidly obscure the relationships between AOD and PM. Furthermore, access to other data describing the atmospheric state is essential in adequately selecting different cases and in building a robust relationship between AOD and $PM_{2.5}$. Such facilities are available at the Cabauw Site for Atmospheric Research (CESAR) which as selected for the study (Figure 2.1).

2.1.1 Cabauw research station

The Cabauw Experimental Site for Atmospheric Research (CESAR) is the focal point of experimental atmospheric research in the Netherlands (http://www.cersar-observatory.nl). The goal of the CESAR initiative is to set-up and to operate an observational facility at the Cabauw site with a comprehensive set of remote sensing and in-situ equipment to characterize the atmospheric column above Cabauw. CESAR is an atmospheric reference site in the European and global research networks and is a collaborative effort of eight institutes in the Netherlands (KNMI, RIVM, TU-Delft, TNO, ECN, WUR, Utrecht University and ESA/ESTEC).

The Cabauw site (51.97 N, 4.93 E) is located in a rural area in the centre of Netherlands. A 213 m metrological tower is used for in-situ monitoring of the atmosphere. A range of instruments measuring parameters related to clouds, radiation, atmospheric state and land-atmosphere interaction are located around this mast. In particular, various remote sensing instruments including radars and lidars are used for atmospheric profiling,

Some of the instruments at Cabauw are also part of instrument networks, such as the lidar which is part of the European Aerosol Research Lidar Network (EARLINET), the radiation measurements in the Baseline Surface Radiation Network (BSRN) and the Aerosol Robotic Network (AERONET). Moreover, Cabauw is being developed as a focal point for air quality studies. Important for our study is the long term time series of AOD and a range of optical and physical aerosol parameters such as size distribution, volatility and aerosol extinction coefficient are obtained. Furthermore, the vertical aerosol distribution is monitored using a lidar. These systems are used within this study and are described in more detail below.

2.1.2 Measurement strategy

A good understanding of the relationship between AOD and PM is crucial, when AOD is used to construct PM maps. To use satellite observations in the particulate matter dossier, artefact-free empirical data are needed to characterise the regionally dependent relationships between satellite AOD and particulate matter, especially for the Netherlands.

In this project, a new set of collocated measurements was obtained of $PM_{2.5}$, AOD (sun photometer), vertical distribution of aerosols from lidar measurements and aerosol measurements at a 200 m observation tower, and various meteorological parameters. In the build-up of this study, a new measurement system for $PM_{2.5}$ was installed at the CESAR site. This new system (Tapered

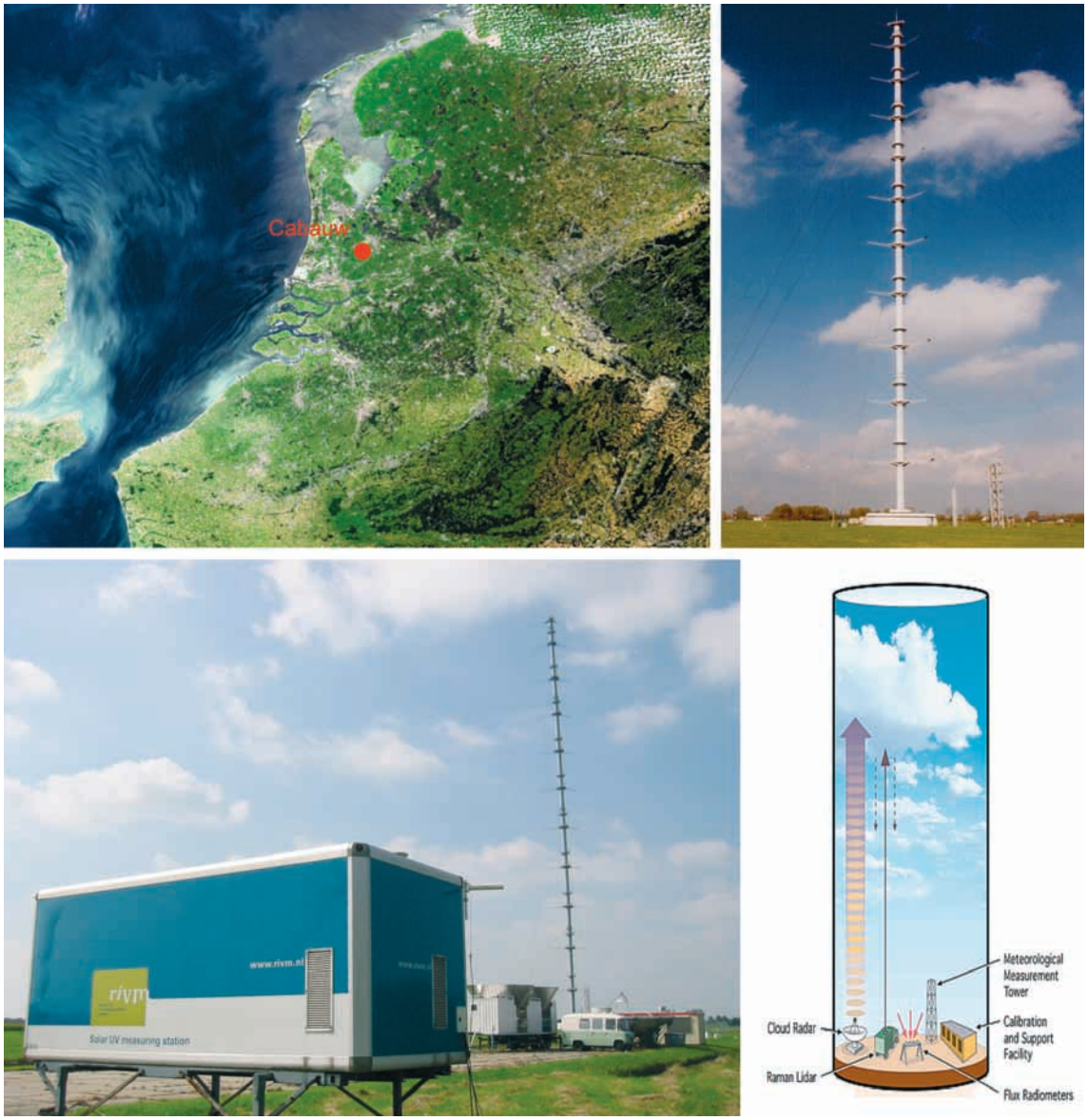

Figure 2.1 Overview of the Cabauw Experimental Site for Atmospheric Research in the centre of the Netherlands. Remote sensing instruments are located close to the 213 m meteorological tower.

Element Oscillating Microbalance with Filter Dynamics Measurement System – TEOM-FDMS) is known to be free of artefacts that result from losses of semi-volatile aerosols during the measurement. Moreover, the CESAR site allows synergy between other instruments installed there. This allows for the determination of the aerosol vertical profile using a lidar and physical and optical characterisation of aerosols, and benefit from other national and international projects such as the EU FP6 infrastructure projects EUSAAR and EARLINET-ASOS. These projects aim at standardisation and harmonisation of the measurements at selected sites, such as CESAR.

The ground-based measurements performed at the CESAR site are summarised in Table 2.1. The main instruments for determining the relationship between AOD and $PM_{2.5}$ are the FDMS-TEOM, the sun-photometer, lidar, and meteorological observations.

Table 2.1 Ground-based measurements performed at the CESAR site

Instrument	Measured quantity	Time resolution
FDMS-TEOM	$PM_{2.5}$	30 min.
Aerosol lidar	Backscatter profile (*)	5 min.
Aethalometer	Black fraction of aerosol	5 min.
Sun-photometer (Cimel)	Aerosol Optical Depth (AOD)	5 min.
Nephelometer	Aerosol extinction at 3 wavelengths	1 s, averaged over 5 min.
OSIRIS, at 3 heights in the 200-m tower and at surface	Proportional to $PM_{2.5}$	10 min.
Meteorological instrumentation	Profiles of relative humidity, wind speed, wind direction, and temperature	soundings: twice daily; tower: seconds-minutes
Long-wave radiometer	Cloud detection	
MARGA	Ammonium nitrate fraction of $PM_{2.5}$	

$PM_{2.5}$ measurements

A TEOM-FDMS (Rupprecht and Patashnick, Model 8500) was installed to monitor ambient $PM_{2.5}$ concentrations (Figure 2.2). It is well known that a standard TEOM underestimates ambient PM concentrations due to evaporation of semi-volatile components from the filter that is conditioned at higher than ambient temperatures. Especially, ammonium nitrate is sensitive to evaporation under these operation conditions. As ammonium nitrate levels are high in the Netherlands (Schaap et al., 2002), the TEOM-FDMS was selected for this study. In a TEOM-FDMS, mass concentrations are obtained from the TEOM that also has a FDMS (Filter Dynamics Measurement System) to examine the behaviour of the mass on the filter under clean conditions. The measurement cycle of the TEOM FDMS is divided into two parts, which are alternated every few minutes. One part of the cycle is similar to the classical TEOM approach, and provides the mass increase due to aerosols. In the second cycle, air passes through a filter that blocks aerosols and then the clean air is led to the TEOM filter. Generally, a mass decrease of the TEOM filter is measured during this cycle, which results from continued evaporation of semi-volatile particulate matter. This is subsequently accounted for in the final result for the total mass of $PM_{2.5}$. Comparisons with reference methods show good general agreement (e.g., Bureau Veritas, 2006). Thus by using the TEOM-FDMS, estimates of $PM_{2.5}$ inline with the reference methods were obtained on a temporal resolution of 30 minutes.

AOD measurements

The aerosol optical depth is routinely monitored using a CIMEL sun photometer (Figure 2.3) and the data are reported to the AERONET (http://aeronet.gsfc.nasa.gov; see Holben et al., 2001). The technical description of the instrument is presented in the Cimel Sun Photometer Manual (http://aeronet.gsfc.nasa.gov). The instrument measures the aerosol optical depth at four wavelengths (440 nm, 670 nm, 870nm and 1020 nm), and the sky radiance in aerosol channels in the azimuth plane (almucantar technique) and in the principal plane. These data are used in the AERONET standard procedures to retrieve information on columnar aerosol characteristics such as the aerosol optical depth, Ångstrøm coefficient and size information. Data processing, cloud-screening algorithm, and inversion techniques are described by Holben et al. (1998; 2001), Eck et al. (1999), Smirnov et al. (2000), Dubovik and King (2000), and Dubovik et al. (2000).

We have used the Level 1.5 data (Automatically cloud cleared but may not have final calibration applied. These data are not quality assured) AOD data in this study are available on a near-real-time basis. The Level 2 data (Pre- and post-field calibration applied, automatically cloud cleared

Figure 2.2 FDMS instrument for $PM_{2.5}$ (a RP 8500 TEOM-FDM) at the Cabauw site

and manually inspected) is updated on an annual basis and became available for part of our observation period towards the end of our study.

Vertical structure of the atmosphere

In the Netherlands, most aerosols are present in the lowest 1 to 2 km of the atmosphere, particularly in the mixing layer. However, it is not uncommon that substantial aerosol-loaded air masses are present above the mixing layer. These aerosols are decoupled from the ground and usually originate from sources far away. They are, therefore, likely to have different (optical) properties than aerosols at ground level. Thus, in-situ measurements of aerosol properties at ground level are not always representative of aerosol particles aloft and the total aerosol column above the measurement site. To be able to recognise such cases, the vertical structure of the

Figure 2.3 A Cimel sun photometer set-up as an AERONET station, including a solar panel for electrical power and a transmitter for relay of data to AERONET headquarters at NASA-GSFC. (Photo: Ed Worrell/KNMI).

atmosphere needs to be known, and particularly about the presence of aerosol layers and clouds. Lidar (Light Detection and Ranging) instruments are well suited to detect aerosol layers, even above the mixing layer.

In this study, extensive use has been made of the RIVM aerosol backscatter lidar. This instrument provides information on the vertical structure of the aerosol profile, atmospheric layering and the presence of clouds up to an altitude of 15 km. A measurement is made at five-minute intervals around the clock. The backscatter lidar operates at a single wavelength (1064 nm) and is therefore limited it its ability to estimate aerosol optical properties in addition to the qualitative vertical aerosol and cloud profile.

2.2 Satellite data sources

2.2.1 MODIS

The MODerate-resolution Imaging Spectroradiometer (MODIS) instrument was launched onboard the EOS-Terra satellite in December 1999. In May 2002, a second MODIS instrument was launched on board EOS-Aqua. The MODIS instruments measure sunlight reflected by the Earth's atmosphere and surface as well as emitted thermal radiation at 36 wavelengths. At least two observations of any place in Europe are obtained per day during daylight hours because the

Terra and Aqua satellites cross Europe close to 10:30 and 13:30 local solar time, respectively. The AOD algorithms for application over land and sea surfaces are mutually independent because the radiative properties of water and land are very different. The retrieval is more accurate over ocean than over land because the reflection by water is relatively low outside the region of direct sun glint, algae blooms and suspended matter, and can be computed accurately from the sea surface wind field.

The MODIS retrieval (v5) of the AOD over land employs primarily three spectral channels centred at 0.47, 0.66, and 2.1 μm. AOD is derived at 0.47 and 0.66 μm, and interpolated to 0.55 μm. The AOD is only retrieved for cloud-free pixels in a 20x20 pixel area at 500m resolution and reported at 10x10km² resolution. Only when more than 12 pixels are classified as cloud-free, an AOD retrieval is attempted. The AOD is retrieved over surfaces that are not highly reflective (thus snow or ice covered surfaces and deserts are excluded).

The basics of the algorithms are described in Kaufman and Tanré (1998) and Remer et al. (2005). The AOD data obtained from these algorithms have been used in numerous studies on the direct aerosol forcing (see, Yu et al., 2006 for a review), aerosol-cloud interactions (e.g., Koren et al., 2005; Wen et al., 2007), source characterisation (Dubovnik et al., 2004; Koelemeijer et al, 2006a), and air quality (e.g., Al Saadi et al., 2005; van Donckelaar et al., 2006; Koelemeijer et al., 2006). Recently, a new collection (collection 5) of AOD data was released. The new algorithms are described in Levy et al. (2007a, b).

In the PARMA project, AOD retrieved by MODIS from the previous collection (collection 4) have been compared with sun photometer data from the AERONET network in Europe. A good temporal correlation was found between MODIS and AERONET. However, a large positive bias of about 50% in the MODIS AOD data was found, which is in accordance with earlier findings. There was a strong seasonal signature in the overestimation of AOD by MODIS with a maximum during summer. After correction for the bias, the accuracy of MODIS AOD retrievals agreed with the pre-specified accuracy of $0.05 \pm 0.20 * AOD$ over land and $0.03 \pm 0.05 * AOD$ over ocean (1-σ level, for individual retrievals) and the residuals show a normal distribution. Furthermore, we hypothesized that, on average, up to one-third of the MODIS retrievals may be cloud contaminated. For some stations in central Europe, this percentage was found to be higher than 50%.

A likely explanation for the strong bias in the MODIS collection 4 data may be found in the treatment of the surface reflectivity. The AOD is only retrieved for cloud-free pixels and over surfaces that are not too reflective. The reflectivity measured at 2.1 μm at the top-of-atmosphere is used to determine the surface reflectivity at that wavelength. Fine-mode particles, which dominate the AOD in most of Europe, have a negligible optical depth at 2.1 μm, allowing almost direct observation of the surface (Chu et al., 2003). In the v4.2 retrievals, the surface reflectivity at visible wavelengths is then obtained by assuming a constant ratio between surface reflectivity at 2.1 μm and that at 0.47 and 0.66 μm. In reality, this ratio depends on surface type and its time-dependent characteristics that determine the reflectivity (e.g., vegetation and soil moisture).

Levy et al. (2007) showed that by using higher surface reflectivity at 0.47 and 0.66 μm, the lowered AOD over land significantly reduced the discontinuity between land and sea over the coastline in the north-east of the USA. In addition, the agreement between MODIS and AERONET improved in that area. A major improvement in the second generation MODIS algorithm (v5.2; Levy et al., 2007) is the inclusion of a pixel-specific wavelength dependence of the surface reflectivity. Compared to v4.2, the surface reflection used in the algorithm has increased over

more vegetated areas in the mid-latitudes (especially in summer). First inspection of the new annual average distribution (see Chapter 6) shows significantly lower AOD over Europe and only slight discontinuities between land and sea areas.

Although the surface reflection is one of the major changes, the differences between the two collections cannot be explained so simply, and more likely results from a combination of factors. The MODIS algorithm (v5.2; Levy et al., 2007) has been updated rigorously. The major changes incorporate the new surface reflectivity assumptions, a new set of aerosol model optical properties derived empirically from AERONET, a new aerosol lookup table and a more elaborate inversion scheme. The cloud screening procedure was not changed. As a consequence of all the improvements, the new product generally yields significantly lower AOD. A preliminary evaluation shows better agreement with AERONET (Levy et al., 2007a). However, the data from the new collection need to be evaluated in detail for Europe. A full evaluation is beyond the scope of the present project. However, we will evaluate the data for the Dutch situation (at Cabauw).

2.2.2 AATSR

Advanced Along-Track Scanning Radiometer (AATSR) instrument onboard the European ENVISAT satellite flies at an altitude of approximately 800 km in a sun-synchronous polar orbit. Like its predecessors, ATSR and ATSR-2, the AATSR has seven wavelength bands in the visible and infrared parts of the spectrum (measurement wavelengths are at 0.55, 0.67, 0.87, 1.6, 3.7, 11 and 12 μm). The instrument has a conical scanning mechanism providing two views of the same location with a resolution of 1×1 km² at nadir view. The radiometer views the surface along the direction of the orbit track at a forward incidence angle of 49° and some 150 seconds later it records a second observation of the scene at an angle close to the nadir view. The swath width of 512 km results in an overpass over a given location – thus a global coverage – every three days at mid-latitudes.

The semi-operational AATSR retrieval algorithm used for SATLINK is based on the scientific ATSR-2 algorithms developed by Veefkind et al. (1998; 2000) and Robles González et al., (2000). It performs a dual view technique over land (see Flowerdew and Haigh, 1995) and a single view technique over water. The aerosol properties retrieved with these algorithms are the aerosol optical depth (AOD) at the available wavelengths (0.55, 0.67, 0.87 and 1.6 μm) and the Ångstrøm coefficient α. The wavelength dependence expressed in σ provides information on the aerosol size distribution. The AATSR dual view algorithm uses both the forward and the nadir view to eliminate land surface reflections from the total reflected solar light measured at the top of the atmosphere. Over land, the surface reflections often overwhelm the aerosol signature, and therefore the dual-view method provides more accurate AOD results than retrieval based on a single viewing angle only. Retrievals are available on the scale of the pixel size of 1×1 km² (Level 2) and averaged over larger scales (Level 3) for European maps. AATSR satellite measurements of the radiation at the top of the atmosphere are input for the semi-operational AATSR aerosol retrieval algorithm. The AATSR swath of 512 km allows for an overpass over each geo-location every three days, between 10.00 and 11.00. The retrieval procedure is depicted schematically in Figure 2.4.

The aerosol model used in this work is an external mixture of anthropogenic aerosol (sulphate/nitrate water soluble) and sea salt. The effective radius of the anthropogenic mode is 0.05 μm. The optical properties used in the retrieval procedure are those applying to anthropogenic water soluble aerosol (Volz, 1972). The sea salt mode has an effective radius of 1 μm and the

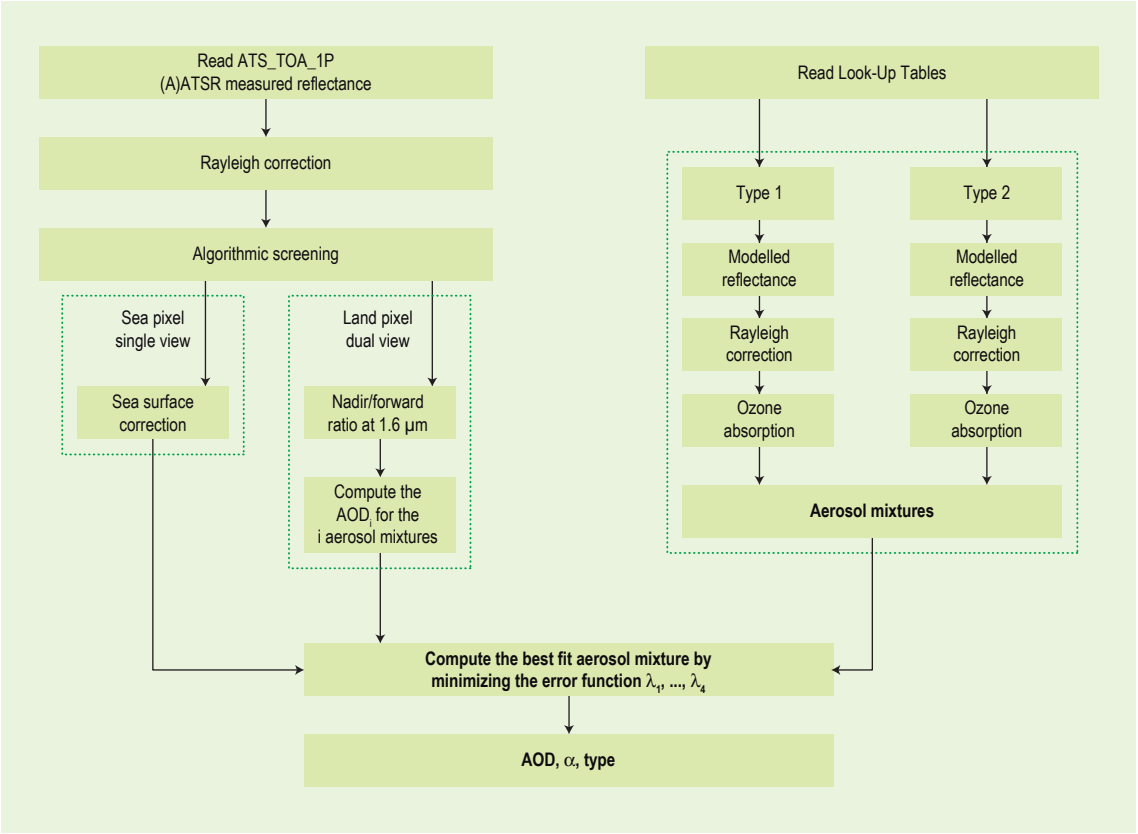

Figure 2.4 Schematic overview of the semi-operational AATSR retrieval algorithm

optical properties were taken from Shettle et al. (1979). A Mie scattering code and the Radiative Transfer Model DAK (De Haan et al., 1987; Stammes, 1994) are used for the generation of lookup tables.

Aerosol properties can only be retrieved for cloud-free conditions and therefore an automated cloud screening procedure is applied based on cloud detection routines initially developed for off-line applications by Koelemeijer et al. (2001), and adapted for automatic applications by Robles González (2003). However, experience in former projects, such as HIRAM, has shown that some enhancements had to be made for improved automated cloud screening and selecting good-quality AOD pixels. By using both channels of AATSR instead of the nadir and the forward channel only, the screening of clouded pixels was stricter and improved.

Furthermore, corrections for ozone, surface contributions and atmospheric (Rayleigh) contributions are computed and finally, the corrected TOA (top-of-the-atmosphere) reflectance at the satellite sensor is compared with the modelled reflectances in iterative steps in order to select the right aerosol mixture. This procedure is based on a lookup table approach. Measured and modelled reflectances are matched using an error minimisation procedure to determine the most likely aerosol mixture and the AOD for the available AATSR wavelengths (Robles González et al., 2000;Robles González, 2003).

2.3 Data processing

Sun photometer
The sun photometer AOD data were obtained from the AERONET site to comply with AERONET standards. The available data are level 1.5 which means that they are fully screened for clouds but that the final calibration of the instrument (needed for level 2.0) and the final (partly manual) checks on the data quality have not as yet been performed. For part of the time series, Level 2.0 data were available just before the end of the project. A preliminary assessment of the influence of the extra checks is given in the discussion, see Chapter 6.

TEOM-FDMS
The TEOM-FDMS provides the $PM_{2.5}$ mass in combination with instrument diagnostics. The instrument has a range of status codes indicating instrument reliability and data validity. We used only data without a reported malfunction or warning code. For these situations, the status code is 0. Furthermore, the concentration had to be positive and all data with a positive correction for the volatile fraction were disregarded. This screening may be too strict, but it refined the selected data to the best available.

LIDAR
From the lidar data, quick look figures were drawn for each day for visual inspection. The backscatter profiles are difficult to use in a statistical procedure. Therefore, a number of variables were computed from the profile data. These include cloud presence (flag), cloud base and integrated backscatter over the lower 1 and 3 km.

Meteorological variables
Standard meteorological variables (T, RH, Wind direction and speed) for the Cabauw site were taken from the CESAR data portal. A classification of the synoptic situation was obtained from the German Weather Service. The classification is available on a daily basis and is discussed in more detail in Chapter 5. All instruments have their own temporal resolution, ranging from minutes to an hour. Thus hourly mean values were computed for all instruments and the meteorological variables (T, RH, Wind direction and speed). Daily data, such as the type of synoptic situation, were assigned to all hours in the day. All data were combined in a single database for use in the analysis.

MODIS
MODIS data were downloaded in HDF format from the MODIS Distributed Active Archiving Center (DAAC).. All MODIS Terra and MODIS Aqua data were obtained that were available for the Netherlands and surroundings in the period for the July 2006-July 2007. The AOD was taken from the HDF data field 'Optical_Depth_Land_And_Ocean' within the MOD04 (Terra) and MYD04 (Aqua) data product, collection 5. The MODIS Aerosol product contains data that have a spatial resolution (pixel size) of 10x10 km^2 (at nadir). Each MOD04_L2 product file covers a five-minute time interval, which means the MOD04_L2 output grid is 135 10-km (at nadir) pixels in width and 203 10-km (nadir) pixels in length for nine consecutive granules. Every tenth granule has an output grid size of 135 by 204 pixels. All MODIS Atmosphere data products are available to the public (at no charge).

AATSR
The AATSR satellite data used during the SATLINK project are orbits of Level-1b top-of-the-atmosphere Gridded Brightness Temperature/Reflectance (GBTR) products. Level-1b is the raw

satellite data calibrated and geo-referenced at a processing and archiving facility (PAF); the GBTB is a gridded brightness temperature product for the infrared channels and a gridded reflectance product for the visible and NIR channel. These data products have been downloaded from the ESA rolling archive servers and stored locally on external HDs for further processing with the aerosol retrieval algorithm.

The AATSR retrieval algorithm automatically selects those orbit segments that coincide with the SATLINK domain. The retrieval output has been stored in ASCII format for high resolution maps (generic 1×1 km² pixel size) with an AOD value for each pixel. A second output product is low resolution maps (10×10 km² pixel size) for AOD, the number of high resolution AOD values in one low resolution pixel, and the standard deviation of the AOD in the low resolution cell. The retrieval algorithm cuts the dataset for the lower and upper 10%, thus discarding outliers that do not contribute to a proper and qualitative high AOD result. Furthermore, post-processing of the data adds an extra restriction on each low resolution pixel dataset by admitting only low resolution AOD values for which the standard deviation is lower than 0.05.

For both MODIS and AATSR, the AOD retrievals were mapped on a grid over Europe with a spatial resolution of 0.125x0.0625 degrees lon-lat, which refers to about 10x10 km².

2.4 Analysis procedure

Data in the database were used to establish the relationship between AOD and $PM_{2.5}$ at Cabauw station. The steps in analysing the data and combine these data with satellite data are described below.

1. Analyse the time-series of AOD from sun-photometer with those of $PM_{2.5}$for a visual inspection of the data, a statistical description of the data and to establish the overall correlation between AOD and $PM_{2.5}$.
2. Select periods with a high and low correlation between AOD and $PM_{2.5}$.
3. Investigate reasons for the low/high correlations found in step 2, using measurement data from other instruments, specifically the lidar observations.
4. Based on step 3, select valid data points representative for periods with a good correlation between AOD and $PM_{2.5}$. Assess how the relationship is influenced by variations in meteorological parameters (such as mixing layer height, relative humidity profile, wind speed, wind direction) and other factors.
5. Based on steps 3 and 4, specify the situations in which AOD can be used to map $PM_{2.5}$, and establish their relationship. This forms the recipe to map $PM_{2.5}$ for the Netherlands.
6. Use the results of the field study to make a link with satellite data. AOD from the sun-photometer at the CESAR site (Cabauw) was compared with that derived from AATSR, and MODIS. This serves as validation of the satellite based AOD and enables the influence of satellite algorithm related effects and other effects on the correlation between AOD and $PM_{2.5}$ to be extracted.

Demonstrate the feasibility by constructing a map of $PM_{2.5}$ for the Netherlands for an appropriate period, using the established relationships between AOD and $PM_{2.5}$.

3 Overview of ground-based data

3.1 Statistics

All instruments were operated from 1 August 2006 to 31 May 2007. A statistical overview of the data obtained is presented in Table 3.1. The average measured AOD was 0.29. The observed range in the level 1.5 data is from virtually zero (0.04) to 2.5, with a median value of 0.25. For Cabauw, a longer AOD record exists as part of the AERONET network since 2005. The AOD observed in this study is slightly higher than the mean value of 0.26 for the period April 2003 to April 2007. The slightly higher mean value is probably due to the use of level 1.5 data as discussed in Section 4.3.

The measured average $PM_{2.5}$ concentration was 18.2 µg/m³, which is higher than in other areas in Europe (Putaud et al., 2004) and confirms that the Netherlands is characterised by a high PM burden. The mean concentration for a full year (August 2006 to August 2007) was 17.5 µg/m³. Thus, the mean $PM_{2.5}$ concentration over the period under study is representative of a full year. For comparison, a limit value is to be set in the new EU air quality directive 25 µg/m³ for annual average concentrations to be met by 2015. Also, an indicative limit value is to be set for 2020 of 20 µg/m³ for annual average $PM_{2.5}$concentrations Maximum concentrations were observed in the last days of March and the beginning of April, with a peak value of 156 µg/m³ (see Figure 3.4).

The FDMS data indicate that the semi-volatile fraction is very important, especially during PM episodes. In Figure 3.1, the measured $PM_{2.5}$ concentration and its semi-volatile component for January to March 2007 are presented. On average, the semi-volatile fraction was about 25% of the total particulate mass. Inspection of the time series indicates that the volatile fraction was relatively constant as function of particulate mass. For example, during the episode at the end of March about 50 µg/m³ of the mass (~150 µg/m³) was found to be semi-volatile. The main semi-volatile component in $PM_{2.5}$ was ammonium nitrate, an important component of PM in north-western Europe (Schaap et al., 2002). The hypothesis that ammonium nitrate constitutes most of the lost mass is substantiated by a comparison between the volatile fraction and chemical characterisation of PM by the MARGA system during January 2007 (see Figure 3.2).

3.2 Initial comparison between AOD and $PM_{2.5}$

During the project, co-located measurements of AOD and $PM_{2.5}$ were obtained for the period from 1 August 2006 to 31 May 2007. As an initial assessment, all AOD data were plotted against the co-located $PM_{2.5}$ data in a scatter diagram (Figure 3.3). Initial inspection shows large vari-

Table 3.1 Statistical overview of the AOD and $PM_{2.5}$ values obtained in this study

	AOD	$PM_{2.5}$ (µg/m³)
Mean	0.29	18.2
Median	0.25	13.0
N	864	3946
Min.	0.04	0.0
Max.	2.45	156.5

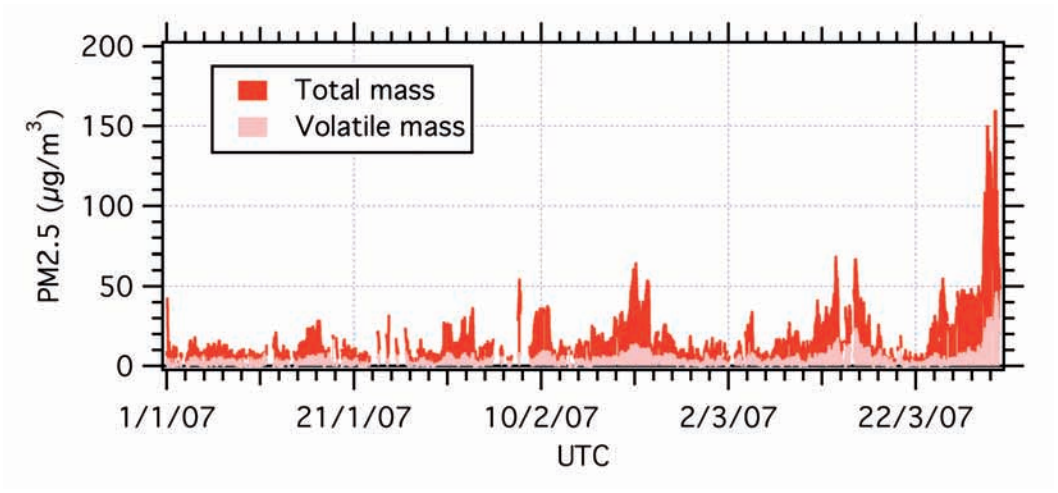

Figure 3.1 Measured concentrations of total $PM_{2.5}$ and the volatile fraction obtained by the TEOM-FDMS for January to March 2007.

ability and no indication of a relationship between the variables. Closer examination shows no combination of low AOD and high $PM_{2.5}$. However, there were many occasions when AOD was high, but $PM_{2.5}$ was very low. In short, a first inspection of all data shows a low correlation (R^2=0.26) between AOD and $PM_{2.5}$.

The complete time series of AOD and $PM_{2.5}$ is presented in Figure 3.4. $PM_{2.5}$ is given as a grey line and the AOD data are superposed as black squares. The AOD values are given on the secon-

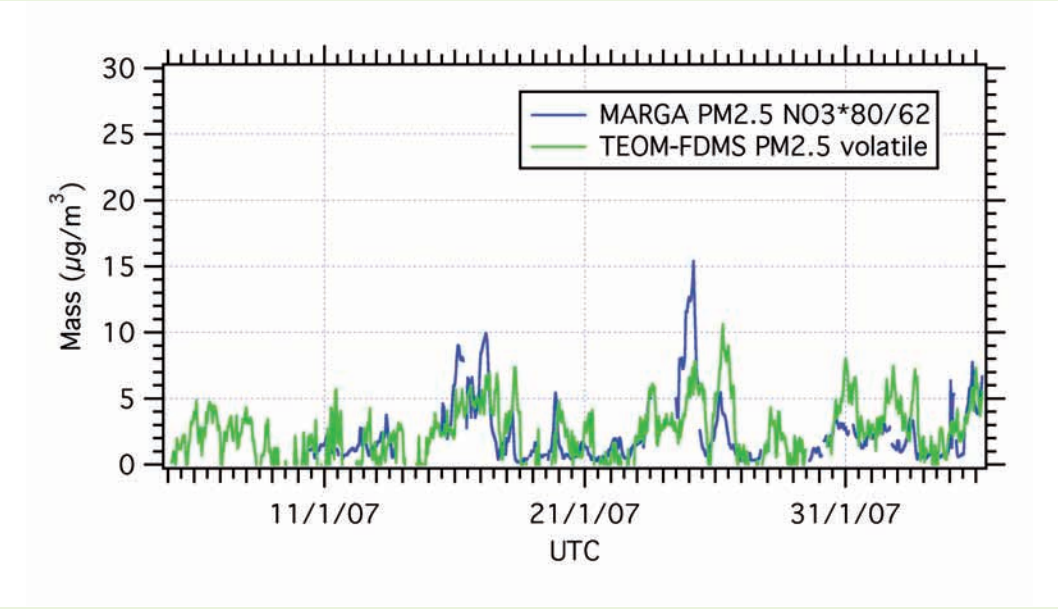

Figure 3.2 Comparison between total volatile mass (FDMS; green) and ammonium nitrate levels (MARGA; blue) for January 2007. Data from the MARGA system were obtained from ECN. The MARGA measurements of nitrate were multiplied by the ratio of molecular masses of ammonium nitrate and nitrate to obtain a measure of the ammonium nitrate contribution to $PM_{2.5}$.

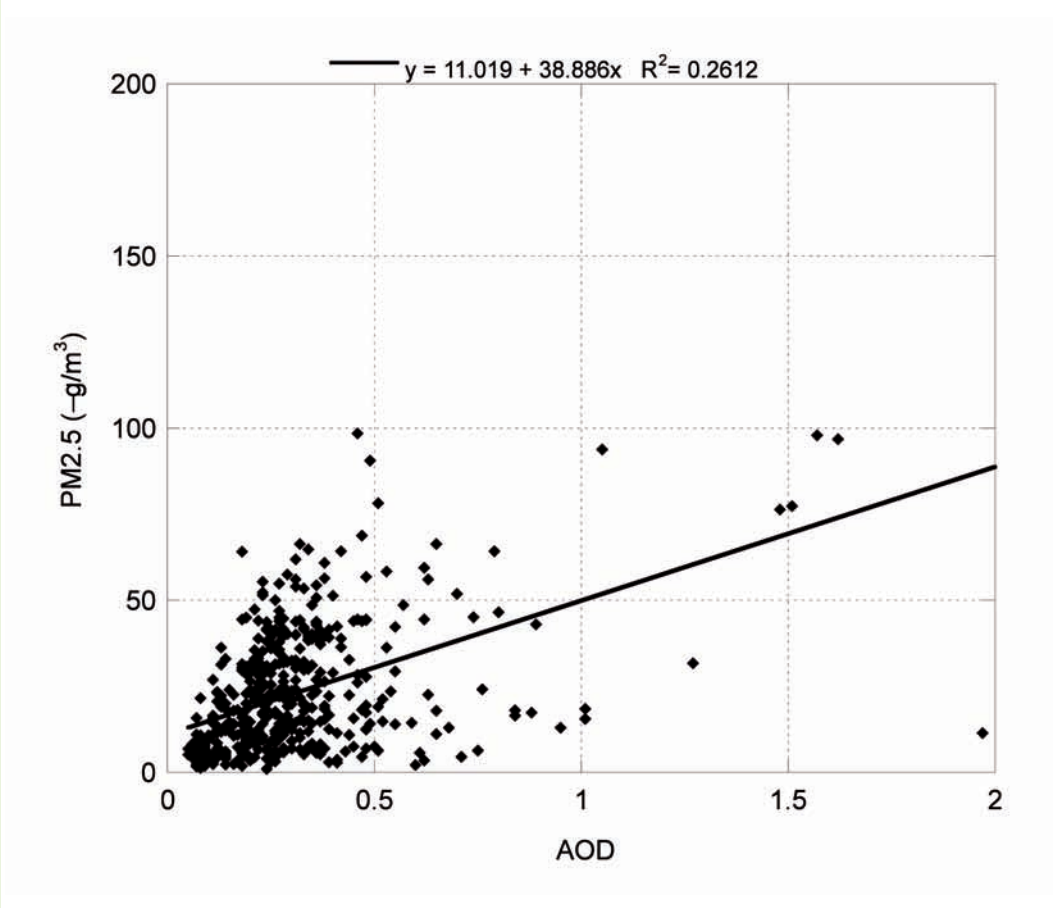

Figure 3.3 Ground-level $PM_{2.5}$ concentration as function of sun photometer AOD (level 1.5) for all combinations during the study period.

dary Y-axis. Visual inspection of the time series provides good insight into the actual data. Moreover, compared to the scatter diagram the information content is much higher. Inspection of the upper panel (August-September 2006) yields a more differentiated picture. During August, $PM_{2.5}$ concentrations were relatively low, whereas the sun photometer yielded high AOD data. The two measures are uncorrelated during this month. In contrast, the AOD and $PM_{2.5}$ data for September track each other well (R^2 =F 0.65).

Inspection for the remainder of the study period confirms that periods with and without correlation follow one another. As well as September, a very promising correlation between AOD and $PM_{2.5}$ was found for a prolonged period between 15 March and 15 May (R^2=0.56). For almost two months (March and April) AOD and $PM_{2.5}$ track on another very well, including the event around 30 March when the highest $PM_{2.5}$ concentrations in the measurement period were observed.

Visual inspection of these time series raises several questions. The most important being why is there a good correlation in some periods and not in the others This was investigated using the lidar vertical backscatter profiles.

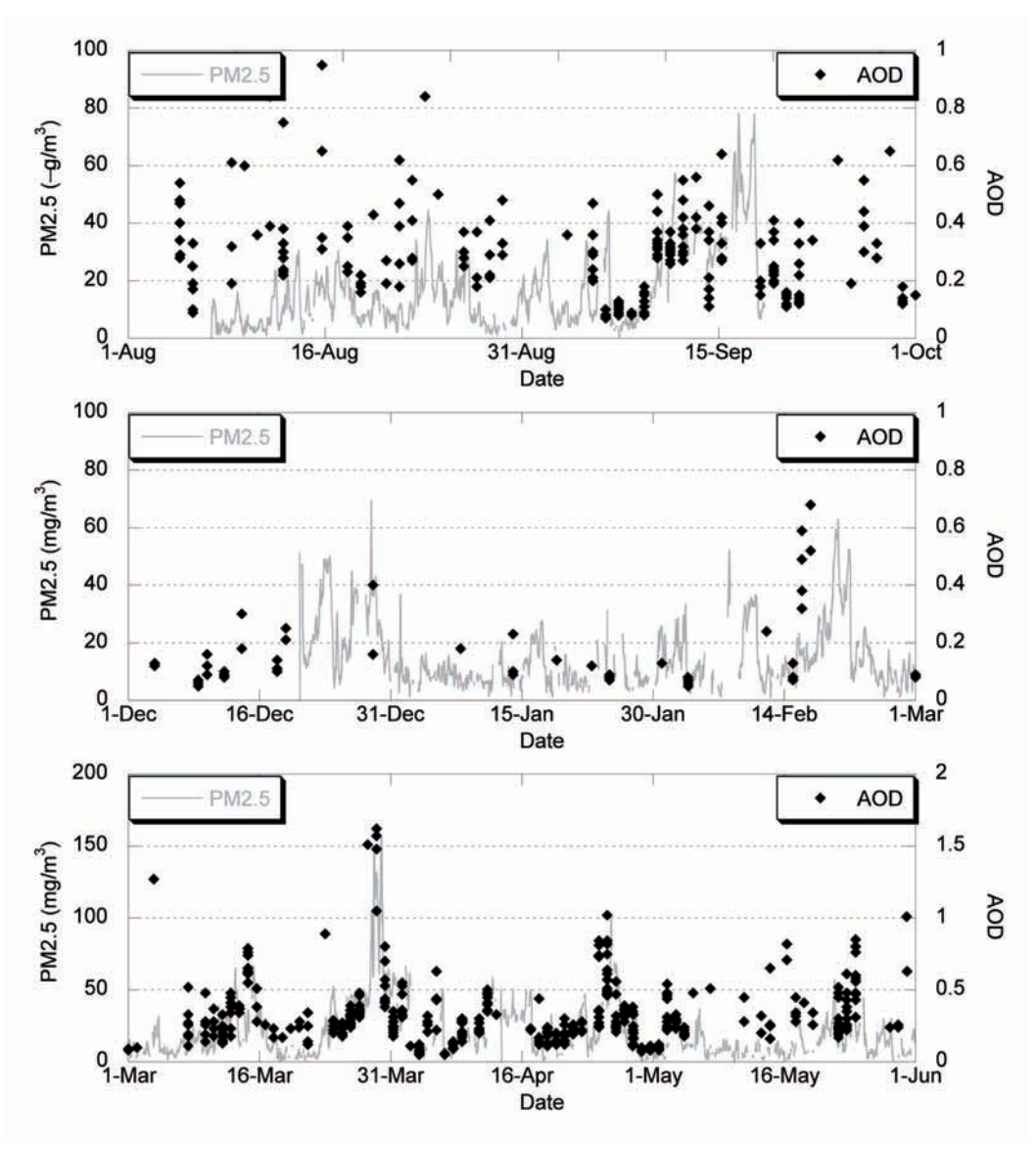

Figure 3.4 Time series for $PM_{2.5}$ and AOD for the period August-September (upper panel), December-February (middle panel) and March-May (lower panel).

3.3 Examples of vertical aerosol profiles

From the visual comparison of time series of AOD and $PM_{2.5}$ in Section 3.2, correlation in August was much lower than, for instance, in September 2006 or March-May 2007. The vertical structure of the atmosphere is shown for two cases; August (Figure 3.5) and September (Figure 3.6). In the time-height lidar plots, the colour scale (in arbitrary units) is representative of the light scattering that occurs at a given height at a given point in time. Dark and light blue hues indicate low scattering, green and brown are indicative for aerosols and white is associated with very strongly scattering particles and clouds. Since the noise level in the lidar data increases with altitude, detection of low scattering levels becomes more difficult at higher altitudes. From these examples, it is clear that presence of clouds probably contaminates the sun photometer AOD measurements and AOD may be overestimated. In such cases, $PM_{2.5}$ values appear lower

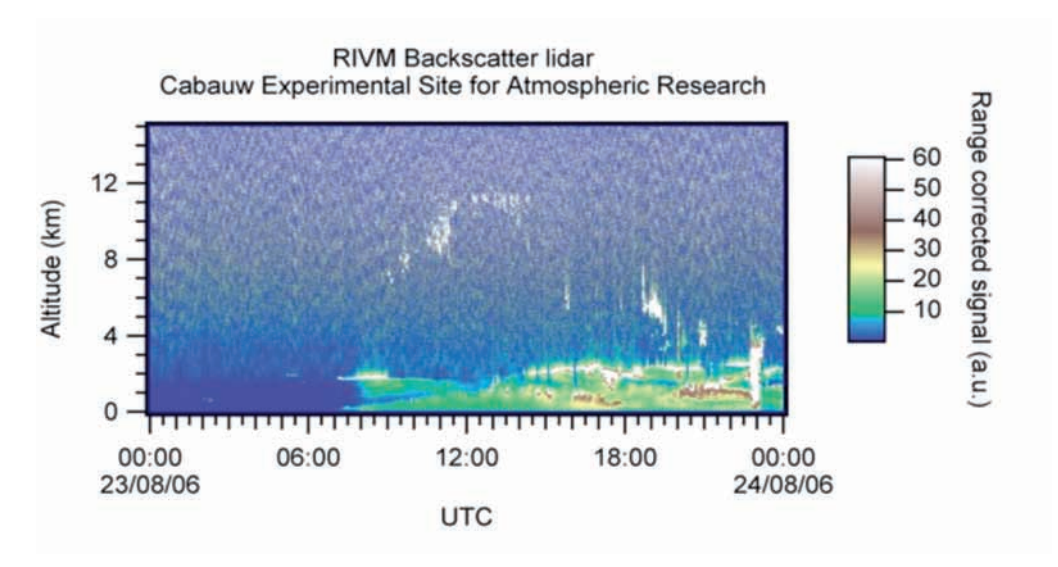

Figure 3.5 Colour coded time-height plot of lidar data for 23 August 2006. Variable clouds at different heights are detected as strongly scattering atmospheric constituents and are depicted in white.

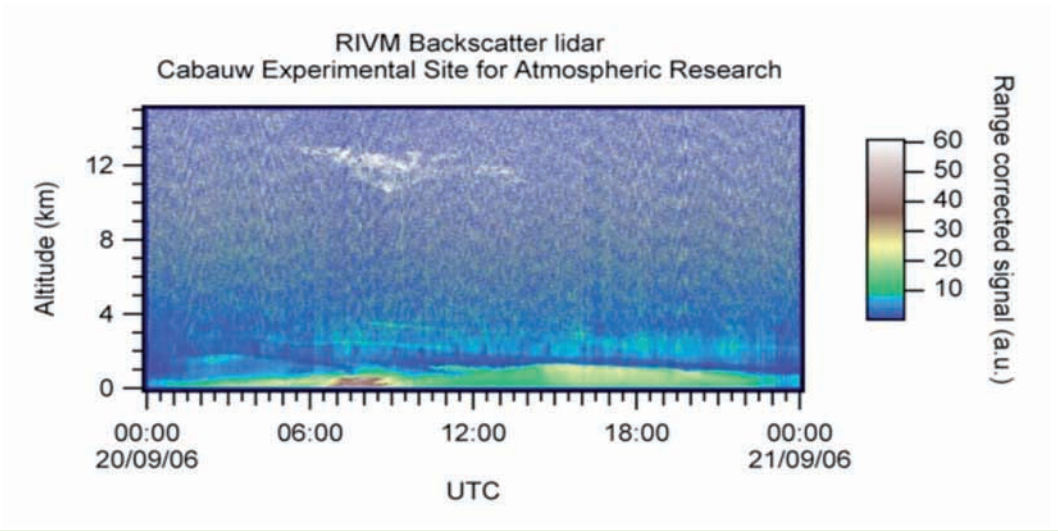

Figure 3.6 Colour coded time-height plot of lidar data for 20 September 2006. This is a typical day with fair weather. Low altitude clouds are not present, but optically thin cirrus clouds are present between approximately 6 and 12 UTC. Also, a lofted aerosol layer can be observed between 3 and 4 km that is decoupled from the mixing layer.

than AOD values. While this may be clear in some cases where high AOD values occur, cloud contamination in the AOD measurements of the sun photometer is less evident with high cirrus clouds that have only low optical depth. In Chapter 4, different measurement methods for cloud detection are described and are applied to screen the sun photometer AOD measurements for cloud contamination.

4 Analysis of AERONET AOD data

In addition to the AOD and $PM_{2.5}$ data, auxiliary data on the state of the atmosphere were collected simultaneously at the Cabauw site. This allowed investigation of disturbing effects of clouds on the AOD measurements by the sun-photometer using these auxiliary data (see Section 4.2), and also investigation of the dependence of the relationship between AOD and $PM_{2.5}$ on atmospheric parameters such as mixing layer height (Section 5). These auxiliary atmospheric parameters are described in Section 4.1 and the effect of cloud contamination and criteria to remove affected data from the data set are discussed in Section 4.2.

4.1 Cloud detection methods

Detection of clouds using lidar data
Lidar systems can be used to detect clouds as they show up as strong scatters in lidar data. Moreover, measurements in cloudy conditions show relatively long time-delay (or 'range' modulations) of the signal caused by multiple light scattering inside the cloud.

A combination of three algorithms was used to detect clouds based on these characteristics. The first approach is a threshold method where the attenuated lidar backscatter signals above a threshold are designated as clouds. This works well for high signal to noise ratios (for low altitude clouds). Favourable results are also obtained in noisy cases when smoothing of the lidar signal is applied. The latter has the disadvantage of reducing (spatial) resolution, but was not a problem in this study because the primary interest is detection of the presence of clouds. Cloud properties are of secondary interest. The second approach aims to detect strong modulations in the lidar signal due to clouds. Thus, the detection algorithm is based on the first order range-derivative as described by Pal et al. (1992). The derivative filter may be set at variable resolution with altitude in order to enhance detection of high cirrus.

These first two approaches only use qualitative lidar signal features. The third approach is more quantitative, and is based on retrieval of the backscatter profile from the lidar data (Klett, 1985) and setting a threshold at the scattering level of clouds. All three techniques were implemented to analyse the data from the RIVM backscatter lidar. A combined approach was finally used to obtain the best possible reliability for cloud detection, including those at high altitudes. Cloud detection was performed for all lidar profiles with five -minute time intervals, thus a maximum of 12 cloud detections was done within an hour.

The lidar detection limit of the backscattered signal is determined largely by the power-aperture product of the lidar (average laser power multiplied by the area of the receiving telescope). Thin cirrus is, therefore, best observed with relatively high-power lidars. Most lidar-ceilometers are not well-suited to observe thin cirrus because of signal to noise limitations. To some extent, this also applies to the RIVM lidar at Cabauw. This may result in either not detecting a cirrus cloud that is present, or in detecting clouds even though the sky is clear(see Figure 4.1). For this reason, our criterion was to flag AERONET data points for rejection in cases of more than three consecutive cloud detections. With three or less consecutive cloud detections, the AERONET data were considered not to be affected by cloud contamination.

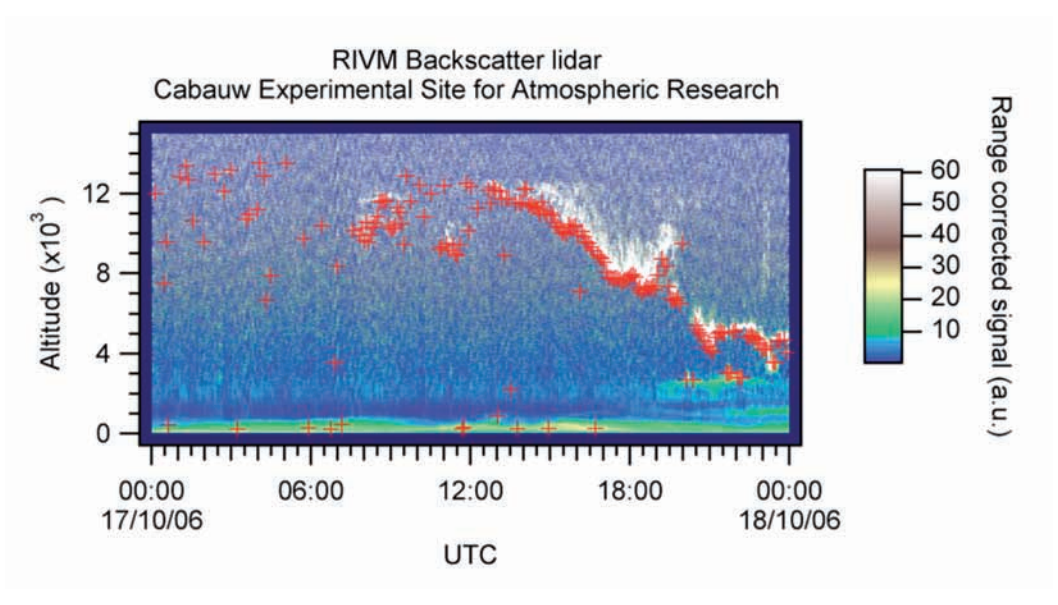

Figure 4.1 Example of cloud detections (red markers) using the RIVM lidar data. In this example, the high altitude clouds are successfully detected but misclassifications also occurred (resulting from noise or aerosols), particularly before the cirrus clouds appear.

Detection of partial cloud amount using infrared radiometer data (APCADA)

A sun photometer obtains AOD data from measurements by looking directly at the sun. Auxiliary data on the atmospheric state should, therefore, preferably be made under the same measurement geometry. Using a lidar only poses two problems:

- A stationary vertically pointing lidar provides vertical aerosol profiles and cloud detection for a small footprint in the zenith sky only. Under some circumstances, the sun photometer observes a clear sky under a slant path, while at the same time the lidar observes a cloud directly overhead, or vice versa. Therefore, additional cloud indicators may be needed to avoid confusion under variable cloud conditions.
- Cloud contamination by optically thin clouds (both high and low-level) may be very hard to detect in sun photometer data. High-level clouds are, however, also difficult to detect using lidar measurements.

For these reasons, the applicability was investigated of a recently developed all-sky cloud cover detection system: APCADA (Dürr and Philipona, 2004). APCADA stands for "Automatic partial cloud amount detection algorithm" that was developed to automate human observations of cloud fraction. The APCADA algorithm was applied to data from the Infrared Radiometer at the Cabauw site. APCADA is based only on measurements of long wave downward radiation, temperature, and relative humidity near to the surface. Using the APCADA method, cloud cover estimates are obtained every 10 minute during the day and night, and it is applicable to radiation stations without knowledge of synoptic cloud observations. APCADA makes no distinction in cloud type (altitude).

APCADA can detect only clouds that have a measurable effect on long-wave down-welling radiation. Thus, APCADA testing of estimated and observed sky cloud cover was restricted to the total amount of clouds without high clouds. Dürr and Philipona (2004) state that further investigati-

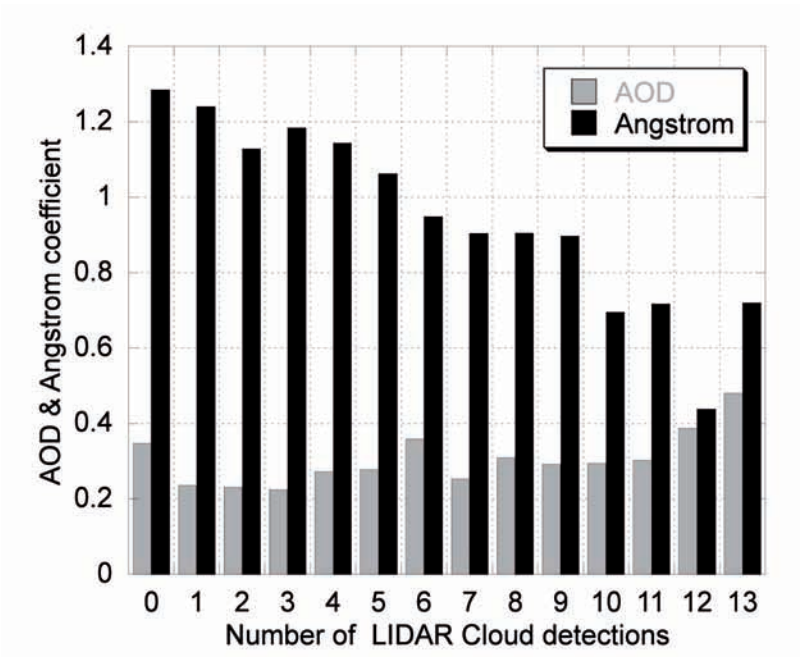

Figure 4.2 Mean AOD and Ångstrøm coefficient as function of the number of lidar cloud detections

ons are needed to combine APCADA with other cloud detection systems during the day and night to include the occurrence of high clouds for climatological studies. APCADA data were provided for this study by KNMI for the full SATLINK observation period.

Detection of clouds using the Ångstrøm parameter

The Ångstrøm parameter indicates the wavelength dependence of light scattering properties of atmospheric particles. For typical aerosols, the Ångstrøm parameter is between 1 and 2, with a medium of about 1.5 in our region (Stammes and Henzing, 2000). For large particles, such as cloud particles, the Ångstrøm parameter approaches zero. The Ångstrøm parameter is obtained from multiple wavelength bands in the Cimel sun photometer. An important advantage of using the Ångstrøm parameter is that it is also a standard product of satellite retrievals of AOD. As shown in Figure 4.2, the average Ångstrøm parameter decreases with an increasing number of cloud detections in an hour. A maximum of 12 cloud detections are possible in an hour, as cloud detections are made at a five minute intervals. An Ångstrøm parameter is expected to decrease with increasing number of cloud detections because cloud particles have a small Ångstrøm parameter compared to aerosols. At a low number of cloud detections, the Ångstrøm parameter is well above unity. This suggests that an AOD data point selection criterion based on the Ångstrøm parameter could be useful to correct for residual cloud contamination. In this study, an Ångstrøm parameter of 1 was used to distinguish between cloud-free and cloud-contaminated AERONET data.

Table 4.1 Statistics of the observed AOD with and without screening for residual clouds using the three cloud detection methods

	Mean AOD	Median AOD	N	Min. AOD	Max. AOD
All data	0.29	0.25	864	0.04	2.45
Lidar (limit 3)	0.27	0.24	376	0.05	1.62
APCADA	0.25	0.23	493	0.04	1.58
Ångstrøm	0.28	0.26	439	0.04	1.51

4.2 Evaluation of cloud indicators

In this section, the atmospheric indicators described in Section 4.1 are used to investigate the dependence of the correlation between AOD and $PM_{2.5}$ on the presence of clouds. This leads to an additional quality screening to remove effects of residual clouds from the AERONET V1.5 dataset of Cabauw. This screened data set was used in further analysis (see Chapter 5).

The impact of the additional cloud screening is shown in Figure 4.3, according to the three screening methods (lidar, ACPADA, and Ångstrøm parameter), and applied to the period August and September 2006. In each panel, the$PM_{2.5}$ time series and AOD measurements are shown. The AOD that passed the additional test are shown as red diamonds, and the data points that failed the tests are shown in black. At first inspection, a significant proportion of the data do not pass the additional tests. For example, almost all data points in August, which was identified as a period without correlation between AOD and $PM_{2.5}$ do not pass the tests and cloud contamination is suspected. The data for September, the first period to show a good correlation between the variables, mostly pass the tests. Most combinations of low $PM_{2.5}$ and high AOD are filtered out with the additional analyses. The cloud detection results from the different methods (lidar, APCADA, and Ångstrøm parameter) do not differ greatly indicating the robustness of the different approaches. Similar results are shown for the period March-May 2007 (see Appendix B).

The statistics of the observed AOD, with and without screening for residual clouds using the three cloud detection methods, are given in Table 4.1. Clearly, the maximum observed AOD decreased after screening for clouds. About half of the sun-photometer observations were excluded after screening for clouds. The impact of cloud screening in the AERONET data was larger than expected. A large number of data points were rejected from the AERONET L1.5 data due to broken cloud conditions, as could be concluded from analysing lidar data. Contamination in the AERONET data resulting from broken clouds was not expected but data contamination resulting from optically thin high cirrus clouds could be expected.

The correlations between AOD and $PM_{2.5}$ after applying the three cloud detection methods are presented in Figure 4.4. The correlation coefficients are R^2=0.44 (lidar), R^2=0.34 (ACPADA), and R^2=0.45 (Ångstrøm). The Ångstrøm and lidar cloud detection methods thus gave rise to almost the same degree of correlation, while the correlation was less using the ACPADA method for the time series.. The lidar method is straightforward, while the Ångstrøm method does not have as pure a physical basis, particularly regarding the criterion of using a threshold of 1 for the Ångstrøm parameter to distinguish between cloud-free and cloud-contaminated AERONET data. Instead, this criterion is tuned to get the best results. This does not mean it cannot be used, but lidar filtering was preferred because it is more straightforward. It may be expected that improvements to lidar signal to noise ratiowould yield better results. Another advantage of using

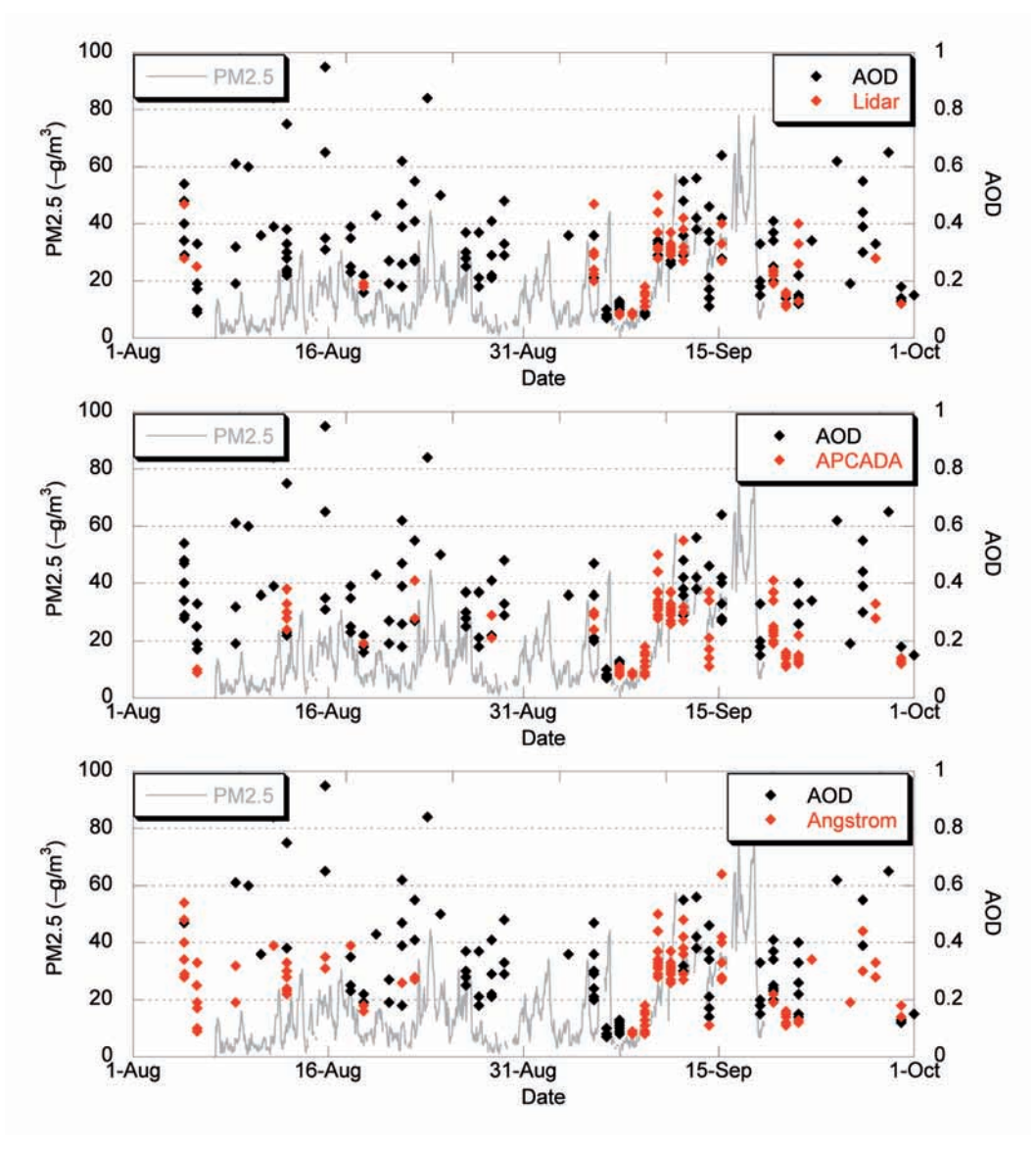

Figure 4.3 Time series of $PM_{2.5}$ and AOD data that are regarded to be cloud free (red) or suspected of cloud contamination (black) for the methodology based on the lidar (upper panel), APCADA (middle panel) and the Ångstrøm parameter (lower panel) for August and September 2006.

the lidar is that information is obtained about the height of the clouds. In the remainder of this study, the lidar screened AOD data were used for further analysis.

4.3 Impact of AERONET v1.5 data

In this study, AERONET V1.5 data for Cabauw were used. The reason is that the version 2.0 data are only processed once a year as it requires the calibration of the instrument and a visual inspection of the data by an expert. In the final month of the project, version 2.0 data were released for Cabauw for the period up until 12 April 2007. The consequences of using the version 1.5 instead of version 2.0 data are presented in Table 4.2.

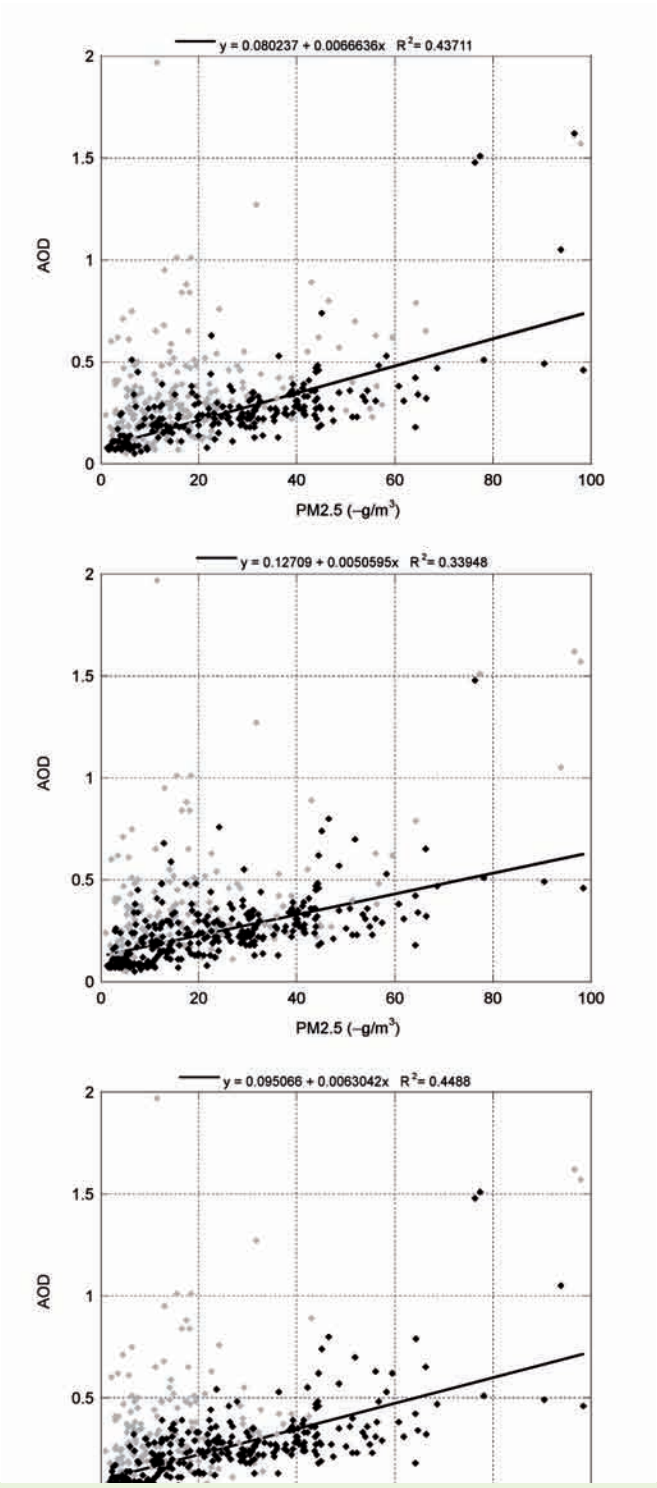

Figure 4.4 Correlation between AERONET AOD and $PM_{2.5}$ measured at Cabauw after screening for residual cloud contamination in the AERONET AOD measurements. Results based on the lidar (upper panel), APCADA (middle panel) and the Ångstrøm parameter (lower panel), for August and September 2006.

Table 4.2 Statistics of the sun photometer AOD data for version 1.5 and 2.0

	AOD V1.5	AOD V2.0
Mean	0.29	0.25
Median	0.25	0.22
min	0.04	0.04
max	2.45	1.62
N	613	482

Comparing AOD data from the two versions indicates that the number of valid data points is significantly reduced by about 20%. Furthermore, the data retained in v2.0 are 98% the same as in v1.5. The other 2% of the data contain a lower AOD in v2.0 than in v1.5. The consequence of the additional screening is that the average AOD is reduced from 0.29 to 0.25, which is considered to be significant.Figure 4.5:

Figure 4.5 shows the correlation between $PM_{2.5}$ and AOD for v1.5 and v2.0. The grey diamonds represent all data, while the black diamonds only show the data that have passed the Lidar cloud screening. Comparison of the versions shows that in v2.0, AOD values above 0.5 that are associated with low $PM_{2.5}$ data, have been eliminated.

As a consequence, the fit between AOD and $PM_{2.5}$ using all data explain a higher percentage of the variability than in v1.5. The black diamonds represent the data after performing the cloud screening using the lidar profiles. Although there are more data points in the AERONET v2.0 than the data set used in this study (lv.15, lidar screened), there was close agreement between the two data sets after our lidar cloud screening. This means that many data points that we independently classified as unreliable were also identified as such in the processing of v2.0 data. This was confirmed by identifying the number of observations as a function of the number of cloud counts per hour (see Table 4.3). The data reduction in v2.0 is about 10% for the hours with a low

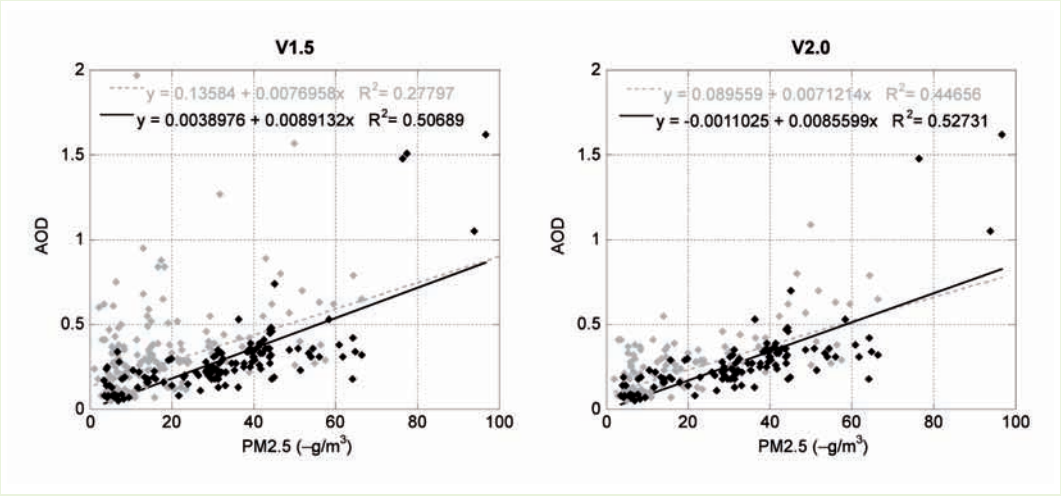

Figure 4.5 AOD as function of ground level PM2.5 concentration for v1.5 (left) and v2.0 (right) for all data (grey) and the data that passed the Lidar cloud screening (black). Data represent the period between the 1st of August, 2006, and the 12th of April, 2007.

Table 4.3 Comparison of the number of observations in the two AERONET datasets (v 15. and v2.0) as function of the number of detected clouds per hour.

LIDAR cloud count	Number of observations V1.5	Number of observations V2.0	Data Reduction (%)
0	103	92	11
1	50	48	4
2	47	40	15
3	36	34	6
4	37	34	8
5	33	28	15
6	40	33	18
7	47	41	13
8	40	32	20
9	35	29	17
10	47	29	38
11	34	17	50
12	59	20	66

number of cloud counts, but increases with cloud count, and sharply increases above nine cloud detections per hour. Since 98% of the values retained in the v2 data set are exactly the same as in v1.5, almost the same dataset was used in our analysis as data set could have been used if v2.0 data had been available. The consistency between the data provides confidence in the use of the lidar as an independent method to address the quality of the sun photometer data.

The shortcomings of v1.5 compared to v2.0 are effectively removed by additional screening for cloud contamination using the LIDAR profiles. Thus, although the analysis is influenced to some extend by the use of v1.5 data, the impact on the relationship between AOD and $PM_{2.5}$ is relatively small.

5 Analysis of the relationship between AOD and $PM_{2.5}$

5.1 Correlation between filtered AOD and $PM_{2.5}$

Testing of additional cloud screening methods for removing unreliable data from the v1.5 data indicates that screening based on the lidar provides the best results. The Ångstrøm parameter is as effective and may provide a good alternative for use in conjunction with satellite data. Comparison to the AERONET level 2 data gives confidence in performance of the additional cloud screening. Thus, lidar cloud screened AERONET L1.5 data was used in further analyses.

Figure 5.1 shows $PM_{2.5}$ concentration as function of the screened AOD data. Using all available data, the following relationship between AOD and $PM_{2.5}$ was found:

$PM_{2.5}$ =F 65.5 * AOD + 10.5 R^2 =F 0.44

where $PM_{2.5}$ is expressed in µg/m³. The slope of the linear fit is rather small, yielding a high cut-off value of 10.5 µg/m³. Considering the combination of AOD =F 0.5 and $PM_{2.5}$ =F 80.0, a slope greater than 100 might be expected. The lower slope is caused by a few data points (4) with AOD values above 1.0. These data points are clear outliers compared to the general pattern.

Each of these data points is associated with the same episode during 29 and 30 March which was characterised by a very high load of the semi-volatile ammonium nitrate. Although the reason for the different behaviour is not known, large uncertainties may be associated with both AOD and $PM_{2.5}$ data under these particular circumstances. Thus, these data points were eliminated from further analysis. The resulting linear fit is:

$PM_{2.5}$ =F 97.5 * AOD + 2.9 R^2 =F 0.40

5.2 Accounting for mixing layer height

The AOD depends on the total vertical aerosol burden, while $PM_{2.5}$ only depends on aerosol burden near the surface. Thus, vertical mixing in a developing mixing layer during a day may dilute $PM_{2.5}$ concentrations, while the vertical aerosol burden remains the same. This suggests that daily variations in the mixing layer height affect the correlation between AOD and $PM_{2.5}$. In a previous study, Koelemeijer et al. (2006) found that the mixing layer height (MLH) affects the relationship between AOD and PM_{10} at most measurement stations in Europe. Whether taking account of the mixing layer height also yields a better defined relationship between AOD and $PM_{2.5}$ for Cabauw was investigated.

The mixing layer is the atmospheric layer in contact with the ground and in which emissions from the ground mix though turbulent mixing (thermally or advectively driven). The mixing layer height varies over time and typically has a diurnal and seasonal cycle. These cycles are clearly observable in backscatter lidar data, since aerosol concentrations are often higher within the mixing layer than in the layers above it. The mixing layer manifests itself in the lidar backscatter data through contrast in aerosol content with other atmospheric layers. Under some

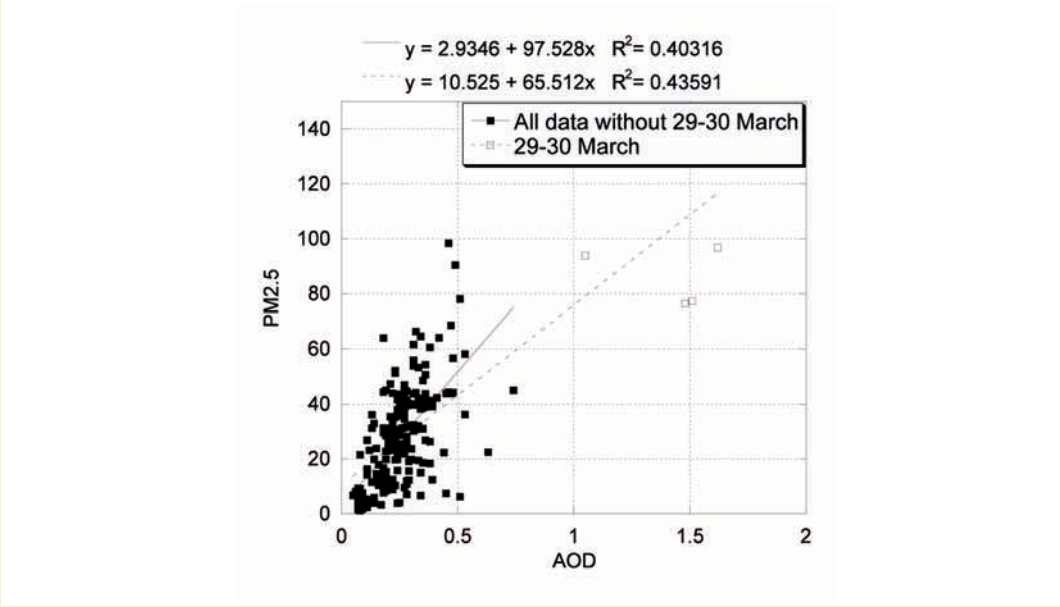

Figure 5.1 $PM_{2.5}$ as function of AOD using all data and those excluding data for 29 and 30 March.

circumstances, remnants of aged polluted layers are present above the mixing layer. These residual layers are not in contact with the ground and are therefore not part of the mixing layer. Because of this, aerosol properties measured in-situ at the ground cannot be regarded as representative of aerosol properties in the lofted layers.

Automatic MLH detection algorithms exist that can be implemented on a variety of backscatter lidars or ceilometers (e.g., de Haij et al., 2007). Such algorithms all have in common that the backscatter lidar data is inspected on vertical gradients in aerosol content (typically going from high aerosol content to low content with higher altitude). Sometimes, persistence of a gradient with time is also taken into account which may add to the reliability of the MLH retrieval. Lofted layers can be recognised similarly.

In this study, the mixing layer height was used as determined from a ceilometer (LD40) at de Bilt, located about 30 km from Cabauw. The reason is that the ceilometer at Cabauw was not operational for most of our study period. The MLH retrieval was performed at KNMI and provided by Dr. Henk Klein-Baltink (KNMI).

Figure 5.2 shows the scatter plot between AOD and $PM_{2.5}$ concentration multiplied by the MLH. The data, however, show that the scatter increases and that the use of the actual MLH does not increase the correlation coefficient. An explanation may be that during periods of stable fair weather conditions, a residual aerosol layer is maintained as identified in the lidar profiles in Figure 3.5. In those cases, a simple multiplication of $PM_{2.5}$ concentrations with the MLH is not expected to improve correlation with the AOD.

In this study, the depth of the mixing layer and the residual layer have been approximated by using the maximum MLH over the last 24 hours. There is less variability in the AOD and $PM_{2.5}$ scatter plot (Figure 5.2) than when the actual MLH is used. However, the explained variability does not significantly increase by using the MLH data in this case. The explanation may be that

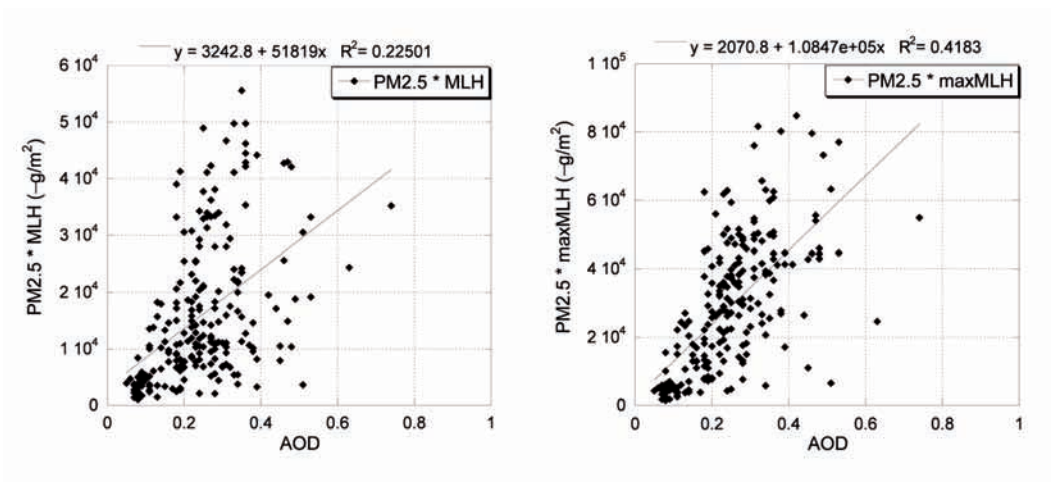

Figure 5.2 Estimated vertical aerosol burden as function of AOD. The burden is calculated using the actual (left) and 24 hour maximum (right) mixing layer height (MLH).

the daily maximum MLH is relatively constant during periods for which AOD data are available (see Figure 5.3). For example, the mixing layer height during September and March-April varied around 1000m. An analysis with ECMWF mixing layer height confirmed the conclusion that accounting for the mixing layer height does not improve the coefficient of determination for the AOD and $PM_{2.5}$ relationship for the time series in this study.

5.3 Sensitivity to the time of the day

While ground-based measurements of AOD and $PM_{2.5}$ are obtained throughout the day, (AOD only during sunlight hours), satellite observations of AOD from MODIS and AATSR are confined to a limited period of the day. The reason is that most satellite instruments aimed to determine the atmospheric composition circle the earth in a sun-synchronous polar orbit. This means that each orbit crosses the equator at the same solar time. Polar orbiting satellites provide full global coverage in 1 to 6 days and pass over north-western Europe at fixed times of the day. Therefore to optimally apply the relationship between AOD and $PM_{2.5}$ as derived from ground-based measurements to AOD measurements of satellites, we investigated whether the relationship changes when data for the window in which the most important satellites overpass are used instead of all available data.

The MODIS and AATSR satellites have their overpasses in the late morning and early afternoon. Here, the data set from all available observations was gradually reduced to observations obtained between 12 and 14 UTC and the AOD-$PM_{2.5}$ relationship assessed.

The effect of constraining the time window is illustrated in Figure 5.4 for the period between 11:00 and 15:00 UTC. Obviously, an overall reduction of available data points is obtained. Also, a high percentage of the points on the edges of the data cloud were observed to be data points associated with early morning or late afternoon measurements. This is especially so for points with low $PM_{2.5}$ and moderately high AOD values. The relationship between AOD and $PM_{2.5}$ as well as the explained variability are presented in Table 5.1. Strikingly, the explained variabi-

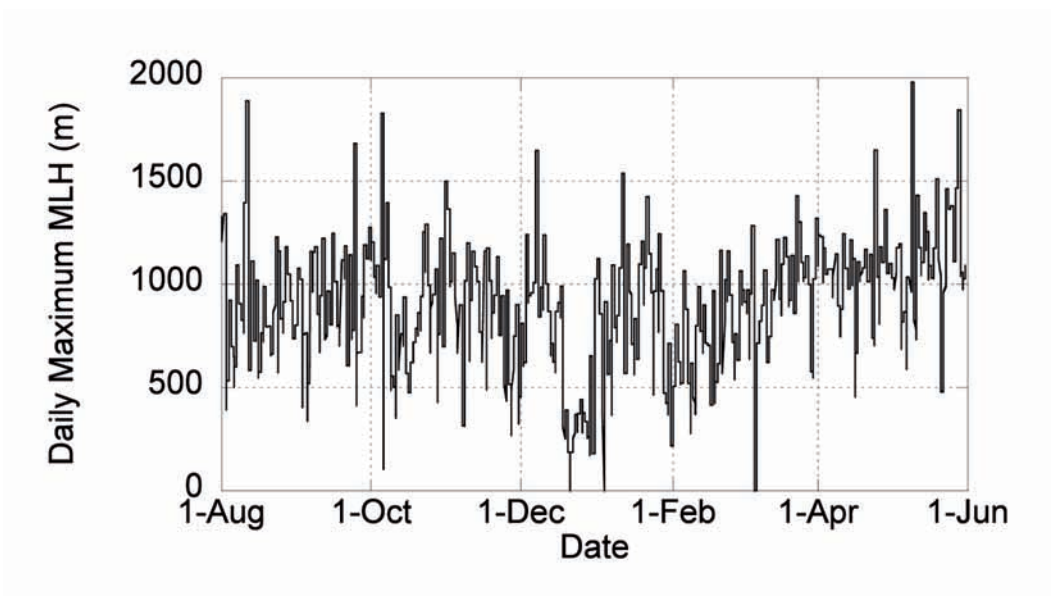

Figure 5.3 Variability of the daily maximum mixing layer height (m) during the study period.

lity rises when the time window is confined towards midday. Also, the slope of the fit increases significantly while the cut-off value decreases simultaneously. Therefore, the influence of forcing the relationship through zero was investigated. These fits yield slopes between 107 and 127, a more moderate increase in slope following a decrease in the time window. By forcing the fit through zero, the explained variability is slightly but insignificantly lower (<1%). Altogether, the fits that are forced through zero show a variability of less than 10% around the central value, thus a more stable relationship between AOD and $PM_{2.5}$ than in case of a two-parameter fit allowing for a non-zero cut-off value.

Several factors may explain the increase in the explained variability when confining the data towards mid-day. During conditions with valid AOD retrievals, the mixing layer height at midday is generally well mixed, without the presence of residual layers.. Another important factor may be related to the solar zenith angle, as a sun photometer is pointed directly at the sun. AOD measurements under large solar-zenith angles (low sun) are associated with much higher relative air-mass factors compared to mid-day. This means that the relative contribution of aerosols in atmospheric layers above the mixing layer may become more important at large solar zenith angles. Furthermore, an averaging effect takes place in the observed aerosol properties and correlation with local observations decreases. Therefore, variability in observed AOD is expected to be higher under small solar-zenith angles. Finally, cloud screening using the lidar is probably more accurate during midday as the lidar profiles the atmosphere directly above the site. Under large solar zenith angles, the observed part of the sky differs between sun photometer and lidar. Greater similarity is obtained under small solar zenith angles.

5.4 Influence of air mass origin

Air pollution conditions as well as favourable conditions for satellite retrievals over the Netherlands are a function of the large-scale meteorological situation. These conditions are normally

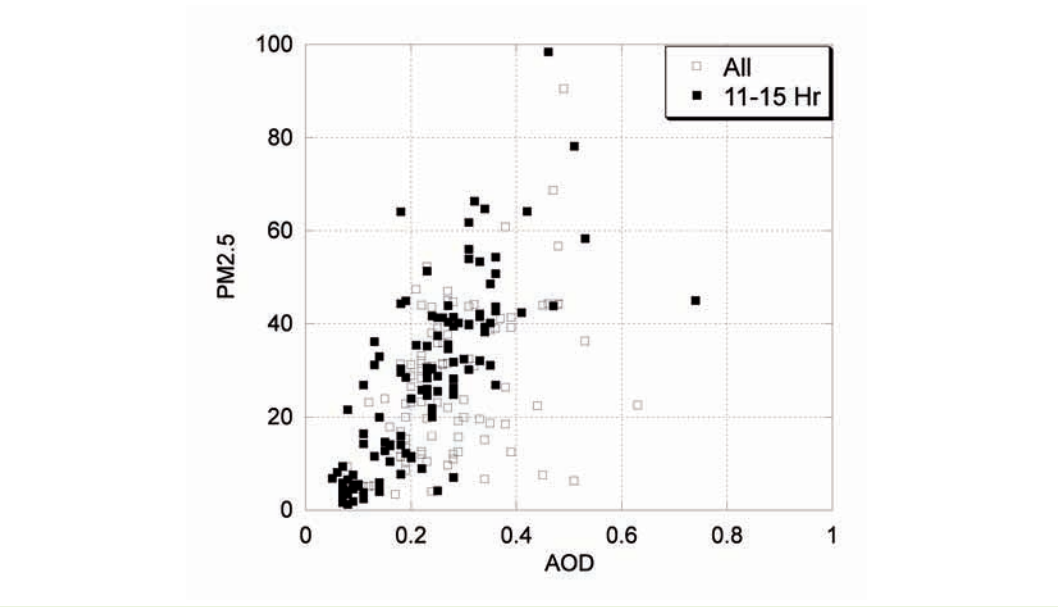

Figure 5.4 Variation of $PM_{2.5}$ with AOD for all data and those between 11:00 and 15:00.

associated with easterly and southerly winds bringing continental air masses to the Netherlands. The origin of the air masses and the meteorological conditions have been addressed by using the classification scheme for synoptic situations from the German Weather Service (REF). This classification system uses four main regimes and 19 different subclasses. This meteorological classification yields a framework to address the air mass origin. Our study addressed the influence of the air mass origin using the four main regimes, as the number of occasions within each of the sub-groups is generally small, except for the most occurring situations.

Figure 5.5 shows the variation of $PM_{2.5}$ with AOD as function of air mass origin. In the Netherlands, the most frequent air mass origin is from the west. However, there are few valid AOD measurements for this wind direction because of the frequent occurrence of cloudy skies in these situations. Moreover, the data do not indicate a positively defined relationship between AOD and $PM_{2.5}$. Northerly wind conditions are mostly associated with clean conditions characterised by AOD lower than 0.1 and $PM_{2.5}$ lower than 10 µg/m³. The classification confirms that high AOD and $PM_{2.5}$ levels are associated with continental air masses arriving from the south, southeast and east. The relationships between AOD and $PM_{2.5}$ for these continental situations are almost identical.

Table 5.1 Relationships between AOD and $PM_{2.5}$ and explained variability as function of the time of day

Time window	$PM_{2.5}$ =F a * AOD + b		R^2	$PM_{2.5}$ =F a * AOD	R^2
	a	B		a	
0-24	97.5	2.93	0.40	107.3	0.40
9-17	111.7	0.55	0.50	113.0	0.50
10-16	106.8	0.96	0.47	110.2	0.47
11-15	124.5	- 0.34	0.57	123.3	0.57
12-14	156.1	- 6.92	0.72	127.8	0.71

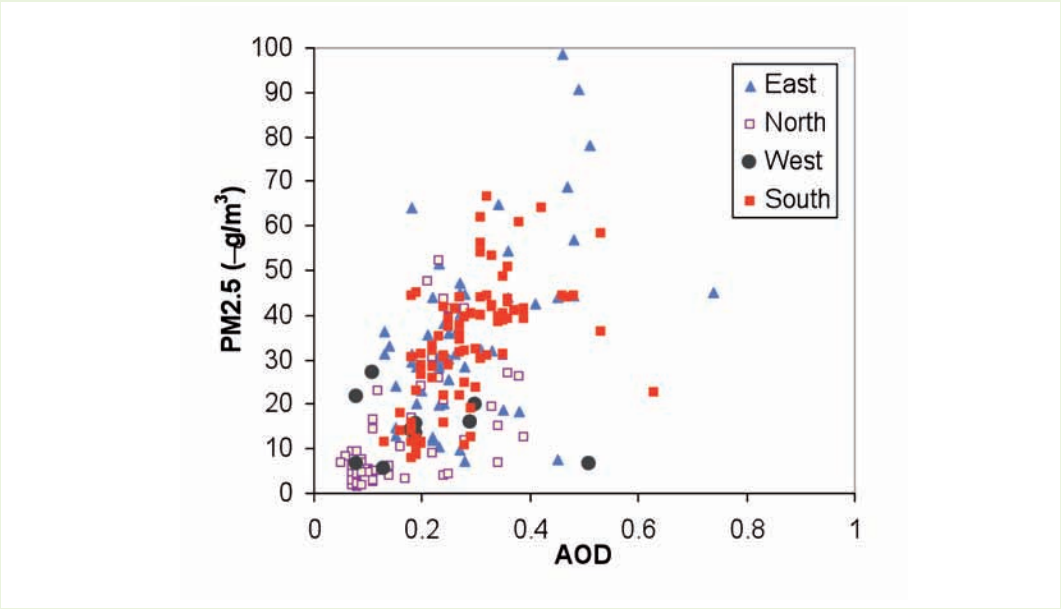

Figure 5.5 Variation of $PM_{2.5}$ with AOD as function of air mass origin.

Although data with an air mass origin from the west have been shown not to have a positively defined relationship between AOD and $PM_{2.5}$, the low number of data do not impact the results presented above. Data for many synoptic situations are too few to provide a basis for statistical analysis. Such an analysis requires a longer time series. In this study, air mass origin as an explanatory variable was not considered further.

5.5 Relationship between AOD and $PM_{2.5}$ at Cabauw - synthesis

In this chapter we have studied the temporal correlation between AERONET AOD and ground level PM2.5 concentration for Cabauw. We refrain to a relationship without the use of the mixing layer depth. This was motivated by the fact that the inclusion of the mixing layer depth did not significantly improve the explained variation of the fits between AOD and PM2.5 at Cabauw. Moreover, retrieving the mixing layer height for large areas and combine those with satellite data (in near real time) complicates the use of such a relationship. Based on the increase of the correlation coefficient obtained using measurement around midday, we arrived at the relationship for the central time window in which the satellites used have their overpasses. The following relationship describes the best-fit between PM2.5 and AOD measured at Cabauw for the data between 11:00 and 15:00 UTC:

$PM_{2.5}$ =F 124.5 AOD - 0.34.

5.6 Discussion

A first inspection of the AERONET (L1.5) AOD and $PM_{2.5}$ data obtained in this study showed a low correlation between the two properties. However, the L1.5 data were contaminated by clouds, and after screening for cloud contamination using lidar data, a better defined relationship

Table 5.2 Overview of AOD-PMx relationships reported in literature. $PM_{2.5}$ is expressed in µg/m3.

Location	PMx	a	b	R^2	N	AOD	reference
Italy	PM_{10}	55	8	0.6	29	AERONET	Chu et al., 2003
France	PM_{10}	-	-	0.27	724	AERONET[1.5]	Pelletier et al., 2007
France	PM_{10}	-	-	0.76	724	AERONET[1.5]	Pelletier et al., 2007
France	$PM_{2.5}$	26	12	0.30	1974	POLDER	Kacenelenbogen et al., 2006)
US	$PM_{2.5}$	22	6	0.40	14000	MODIS[4]	Engel-Cox et al., 2004
US	$PM_{2.5}$	31	5	0.42	19	MODIS[4]	Engel-Cox et al., 2006
US	$PM_{2.5}$	71	XX	0.49	1095	MODIS[4]	Wang and Christopher, 2003
US	$PM_{2.5}$	29	9	0.37	1092	MODIS[5]	Gupta and Christopher, 2008

was obtained between AOD and $PM_{2.5}$ during periods of stable fair weather conditions. During these conditions, continental air masses are transported over the Netherlands. Further analysis showed that the availability of lidar measurements in conjunction with the CIMEL AOD data was valuable for this study. The complementary use of lidar data was also identified by Engel-Cox et al. (2006) who used the lidar data to calculate the aerosol extinction within the mixing layer. After all steps in our study, the explained variability in the relationship between AOD and $PM_{2.5}$ increased. Finally, the following relationship was used to estimate the $PM_{2.5}$ concentration from AOD retrievals:

$PM_{2.5}$ =F 124.5 AOD - 0.34

with $PM_{2.5}$ in µg/m³. Several studies report on the relationship between AOD and PMx; the results are summarised in Table 5.2. First inspection of these studies shows that the relationships reported in the literature are very different as can be deduced from the large range in slopes, cut-offs and explained variability. The slopes reported in literature vary between 19 and 71. The cut-off ranges between 0 and 12, where the lower cut-offs are generally associated with a steeper slope.

The relationships derived in the study based on the AERONET and MODIS data clearly indicate a higher slope than in other studies. On the other hand, the explained variability is the highest for all studies that do not use a statistical model as provided by Pelletier et al. (2007). The major variables that may explain the variability between the reported relationships are discussed below.

The comparison of relationships between AOD and $PM_{2.5}$ may be influenced by the atmospheric conditions during the study. Thus, studies that focus on longer study periods are likely to find more robust results without the influence of special conditions. Thus, continuous monitoring is mandatory. For this reason, $PM_{2.5}$ monitoring at Cabauw will be continued as part of the Dutch Air Quality network operated by the RIVM. Besides the study period, simple issues such as alternative approaches to derive the best fit between AOD and $PM_{2.5}$, and whether or not to force the fit through zero, may explain part of the variability between the available studies. However, other more fundamental issues hamper direct comparison of reported relationships:

Aerosol type, climatic conditions and study period
- Use of AERONET level 1.5 as opposed to level 2.0
- Use of different satellite products

- Use of different PM characterisation.
- The potential impact of these issues on the reported relationships is discussed below.

Aerosol type, climatic conditions and study period

The total AOD is a function of the aerosol column burden and optical properties of the aerosol which depend on the composition and size of the aerosols. Thus aerosol type such as marine, remote continental or polluted continental and different mixtures of these types are expected to yield different relationships. Our study was performed for polluted continental conditions. In these cases, the aerosol in the Netherlands is characterised by high levels of secondary inorganic components, especially ammonium nitrate, and carbonaceous particles. The relationship is thus not readily applicable to other parts of the world.

Several studies report on the AOD-$PM_{2.5}$ relationship over the USA using sites from the monitoring network IMPROVE (e.g., Al Saadi et al., 2003; Engel-Cox et al., 2004). The correlation between AOD and $PM_{2.5}$ is reported to be reasonably high in eastern part of the country, but low in the west of the country. These studies provide a good example for the regional applicability of the AOD-$PM_{2.5}$ relationship as both aerosol types and the climatic conditions differ in these parts of the USA.

Another important parameter for the slope of the relationship is the characteristic mixing layer height at the location. Considering an AOD due to one well mixed layer, the slope of the relationship is inversely proportional to the layer depth. The scale height of this layer around Cabauw is found to be relatively constant and about 1 km. Deeper layers as expected during summer in the USA and in southern Europe would yield a considerably lower slope. In addition, in areas where the scale height is more variable, accounting for it may have a positive impact as has been shown by Koelemeijer et al. (2006a ; 2006b).

The season for which the study is performed is an important factor because the season determines the typical mixing layer height. Furthermore, source strengths of particles, such as those of combustion, and secondary formation routes depend on the season. Hence, the aerosol mix and therefore the optical properties may vary seasonally. This could not be identified for our dataset but that may be specific to the Cabauw site.

Using AERONET level 1.5 versus level 2.0

First analysis of the data showed a relatively large number of points with a high AOD and low PM2.5 concentration. Using the lidar we could identify that the cloud screening of the level 1.5 data does not recognize all clouds as such. An assessment using level 2 AERONET data showed that the final screening of level 1.5 data in the AERONET procedure, which is partly performed by expert judgment, removes a large number of data points identified as susceptible to cloud contamination. Moreover, this final check only removes about 10% of data that our cloud screening did not identify and remove. Hence, after applying our lidar cloud screening to both data sets, almost the same data set is left for use in the analysis.

The consistency between the data provides confidence in the use of the lidar as an independent method to address the quality of the sun photometer data. The shortcomings of v1.5 compared to v2.0 are effectively removed by additional screening for cloud contamination using the lidar profiles. Without co-located lidar measurements, level 2.0 data from AERONET should be used. The comparison between the use of AERONET level 1.5 and 2.0 showed that the level 2.0 contain

less combinations of low $PM_{2.5}$ and high AOD. Thus, as shown in this study, use of level 2.0 data leads to increased slopes, lower cut-offs and a higher explained variability.

Use of different satellite products

Satellites use different instruments to perform the optical measurements. These instruments may use different wavelengths, use one or more views and the resolution for which the data are available may vary considerably. Moreover, independent retrieval algorithms dedicated to the instruments design are used. The algorithms include cloud screening algorithms, aerosol type selection and their optical properties, methods to account for surface albedo and inversion techniques. While AOD products from different satellites tend to be similar with regard to global distribution, large systematic differences are found when zooming in on specific areas such as the Netherlands (e.g., Liu et al., 2005; Kokhanovsky et al., 2007). The sensitivity to the retrieval algorithm is illustrated for the MODIS satellite, which has mostly been used to address the AOD-$PM_{2.5}$ relationship.

The earlier studies (Engel-Cox et al., 2004; 2006; Wang and Christopher, 2003) using MODIS AOD listed in Table 5.2 have used collection 4 data. Our study used the newer collection 5 data. The algorithms underlying the collection 5 data have changed drastically, causing lower AOD to be retrieved in mid-latitudes, especially during summer. For stations in the Netherlands and Belgium, the collection 4 data showed a positive bias of 50 % (Koelemeijer, 2006a; Schaap et al., 2008). For collection 5 at Cabauw, an average bias of -25% was found. Thus, as MODIS AOD has about halved in the Netherlands by the change in retrieval algorithm, this can also explain a large part of the higher $PM_{2.5}$ mass per unit AOD found in our study.

Use of different PM characterisation

The size fraction of PM is a key issue. Using PM_{10} in stead of $PM_{2.5}$ should yield a steeper slope, assuming that the coarse fraction contributes less to AOD than the fine fraction does. This assumption is valid for most of Europe where the $PM_{2.5}$ to PM_{10} ratio tends to be above 0.5 (Putaud et al., 2004). Furthermore, systematic differences between PM sampling techniques associated with both automated equipment as well as filter measurements may cause variability in the reported relationships. Similarly, whether hourly or daily mean PM measurements are used also affects the relationship. Engel-Cox et al. (2006) show that especially the explained variability decreases when daily mean concentrations are used.

In short, the relationship between AOD and PM observed in one region cannot easily be extrapolated to another region, because the aerosol sources and mixtures vary regionally. The strength of the AOD-PMx relationship may also vary due to region-dependent factors but we have shown that the approach used to quantify the relationship is a key aspect to improve the coefficient of determination.

6 $PM_{2.5}$ estimation from satellite AOD

The relationship derived in Chapter 5 is applied to satellite retrieved AOD to estimate $PM_{2.5}$ distribution in the Netherlands and direct surrounding. Firstly, the annual mean satellite derived AOD from AATSR and MODIS, respectively is presented and then validation of these products against the sun photometer data at Cabauw. Finally, the $PM_{2.5}$ fields are estimated and discussed by comparing $PM_{2.5}$ measurements at other locations in the Netherlands.

6.1 Satellite derived AOD fields

The satellite retrieved AOD distributions over the Netherlands are presented for both AATSR and MODIS. The composite maps for the study period are shown in Figure 6.1. It is well known that PM10 levels in the north-east of the Netherlands are generally lower than in the south, and that highest levels are observed in the vicinity of the larger cities as well as in areas of intensive agriculture (Matthijsen et al., 2007). Both the AATSR and MODIS maps of AOD show, however, distinctly different spatial distributions. In the upper panel, the AATSR map shows values of 0.2 to 0.25 over most of the Netherlands. The AASR map shows very little gradients over the Netherlands and surroundings. Surprisingly, slightly higher AOD values up to 0.3 are detected over the north-east of the Netherlands. As for AATSR, the MODIS AOD in the central part of the Netherlands is about 0.2 to 0.25. On both maps, all grid cells with more than 10% surface water coverage are excluded, as these pixels suffer from a clear overestimation of AOD. At land-water boundaries, application of the land algorithm to patches of sea or ocean is likely to lead to too high AOD values (Chu et al., 2002). Furthermore, suspended sediments in shallow water may give rise to high AOD retrievals (Robles Gonzalez et al., 2000; Chu et al., 2002; Ichoku et al., 2005). This hampers interpretation of the spatial distribution of satellite-based AOD over much of the Netherlands, as inland water bodies (rivers, lakes) can also give rise to similar measurement artefacts. The MODIS data show high AOD maxima over the Ruhr area and in Northern France. Minima in the AOD distribution are detected over hilly forest regions in Belgium and Germany, such as the Ardennes. These features are likely to be more realistic, and less affected by the presence of surface waters. Overall, the distributions of AATSR and MODIS are quite different. The AATSR map of AOD shows hardly any structure across the Netherlands. In the MODIS map, the recognition of the Ruhr area and the Ardennes gives some confidence, but the spatial distribution of AOD over the Netherlands seems to be affected by systematic errors, particularly near the coast and large water bodies (rivers, lakes), as is the case in the AATSR data. The spatial dependence of systematic errors in the satellite AOD data could not be studied for the Netherlands, as only independent AOD data are available at Cabauw. In this study, the comparison of satellite measurements of AOD with ground-based measurements was, therefore, limited to the Cabauw site, and is presented in the next section.

6.2 Satellite data evaluation

The MODIS and AATSR AOD distributions show distinctly different gradients over the Netherlands and surroundings. The sun photometer AOD data for Cabauw were used to make a first assessment of the data quality. For a cloudless sky (i.e. for cloudless pixels), a satellite retrieved signal can be compared to a sun photometer signal. For this, co-located data within one hour of the satellite overpass were used. The MODIS instruments both provide a daily coverage over the

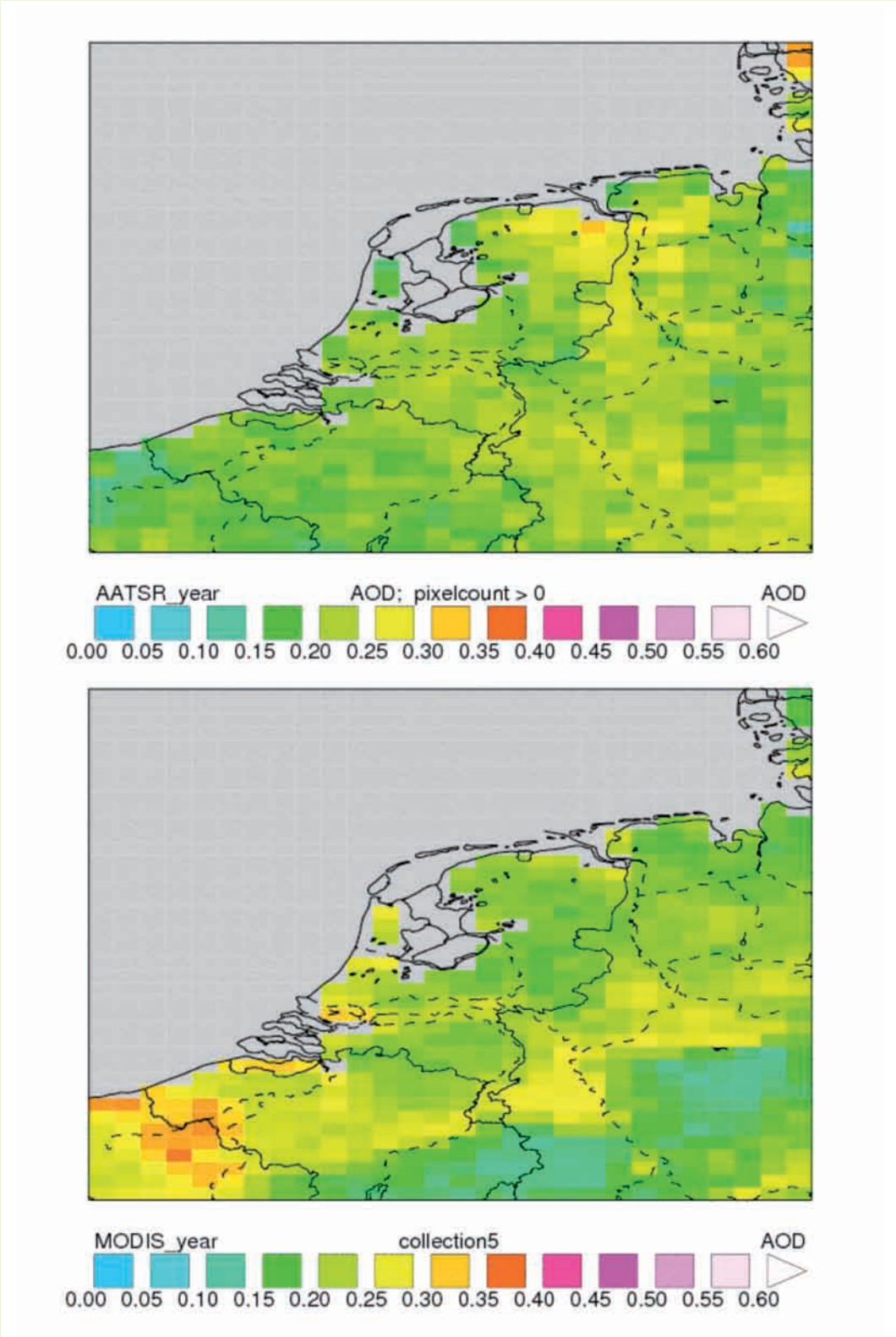

Figure 6.1 AOD composite map based on AATSR (upper panel) and MODIS (lower panel) for the period July 2006 to June 2007. In both maps, all grid cells with more than 10% surface water coverage are excluded, as these pixels suffer from clear overestimation of AOD.

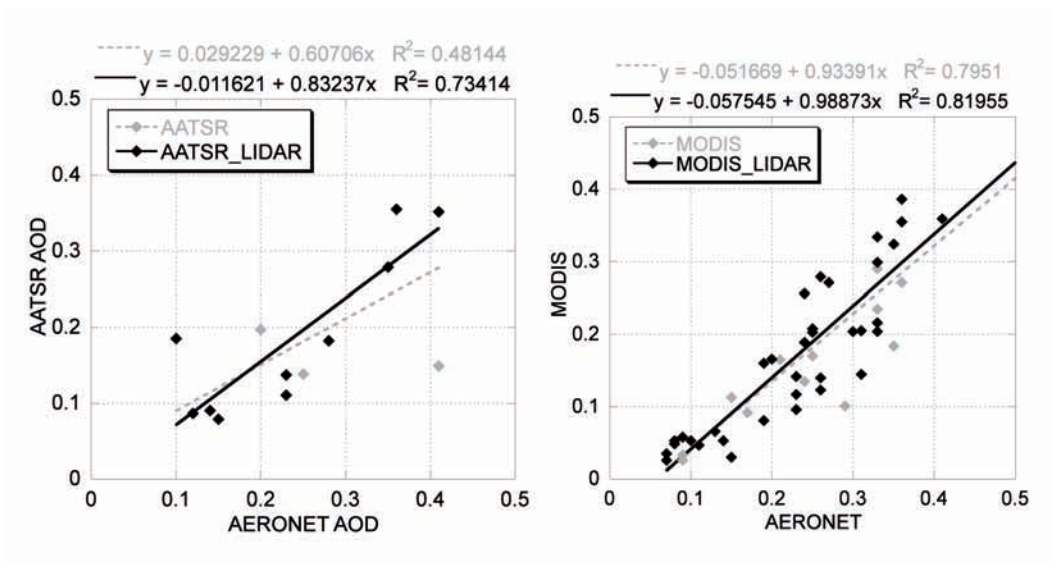

Figure 6.2 Validation of AATSR (left) and MODIS (right) against AERONET at Cabauw. Grey diamonds show all data, and data pertaining to situations where the LIDAR indicates clear sky conditions are shown in black.

Netherlands, whereas AATSR passes over once every three days on average. As a consequence, the set of collocated AOD data is sparse for AATSR as is apparent in Figure 6.2.

The AATSR and MODIS AOD data representative for the 10x10 km² area around Cabauw are compared to the CIMEL AOD measurements in Figure 6.3. We show both the comparison for all collocated data points as well as the CIMEL data that were screened for clouds. For AATSR, the low number of data points prohibits drawing strong conclusions. However, the lidar screened data appear to be slightly below the one to one line, except for one point where AERONET gives an AOD of 0.1. For MODIS, both comparisons indicate very similar results. The MODIS data are slightly lower than those obtained at the AERONET site Cabauw. On average, the bias is 0.05. Nevertheless, the MODIS AOD data show very good temporal correlation, explaining 80 % of the variability measured from the ground. The slope of the regression between the data is very close to 1, indicating that the underestimation is systematic. The standard deviation of the difference between MODIS and AERONET data is about 20%, which is in agreement with other studies.

The validation with AERONET is by definition biased to situations where both the satellite retrieval as well as the AERONET cloud screening identify a cloud-free situation. Situations in which only one of the two retrievals identifies a cloudy situation were not taken into account. The influence of cloud contamination on the AOD climatology by the satellites was not addressed above. Therefore, the number of AATSR and MODIS retrievals over Cabauw were assessed, which do have a satellite AOD value but miss an AERONET retrieval. In this way, we determined the number of observations that could erroneously be identified as cloud-free in the cloud detection procedure of AATSR and MODIS. The results of this analysis are shown in Table 6.1. The table shows that AATSR has 8 out of the total 21 valid retrievals without an AERONET value, where MODIS has 7 out of the total 57 valid retrievals. This suggests that MODIS AOD data are less affected by cloud contamination than the AATSR AOD data are.

Table 6.1 Number of satellite retrieved AOD data with and without co-located AERONET observations. The values in brackets indicate the AERONET data with additional cloud screening based on the lidar data.

	AERONET	
	Yes	No
AATSR	13 (10)	8 (11)
MODIS	50 (36)	7 (21)

Considering the AERONET data with additional cloud screening by the lidar, more AERONET data are classified as cloud contaminated. For MODIS 14 retrievals are present where the lidar indicates that there is possible cloud contamination in the sun photometer data. Hence, it may be that the MODIS cloud screening is not sensitive to the same cloudy situations as the sun-photometer. In these conditions it may also happen that clouds occur in the line of sight between the sun and CIMEL, whereas more than 12 pixels above and around Cabauw were identified to be cloud-free, which allows a MODIS retrieval. Furthermore, our lidar cloud screening is not optimal and this analysis may highlight the occasions where our additional cloud screening is too strict. Similar behaviour is found for the AATSR data.

In short, the percentage of possible cloud contamination is high for AATSR and appears to be lower for MODIS. Combined with the fact that MODIS has many more data points with at least the same performance as AATSR, MODIS data were preferred to AATSR for a first mapping exercise. For the use of AATSR, a validated multi-year composite appears to be required to give a meaningful result.

6.3 Satellite AOD versus ground level $PM_{2.5}$

The focus has been on determining the relationship between AOD and ground-level $PM_{2.5}$ using in situ data for Cabauw. The same analysis can be performed on the basis of the satellite-derived AOD. The variability of $PM_{2.5}$ as function of MODIS AOD is shown in Figure 6.3. For MODIS, the regression line is described by $PM_{2.5}$=120*AOD+5.1, where $PM_{2.5}$ is expressed in µg/m³.

The scatter is reasonably large but the fit explains 52 % of the variability in $PM_{2.5}$. The relationship for the MODIS AOD compares surprisingly well with the relationship determined with sun photometer data. This is especially the case considering the slope is within the determined range with the sun photometer and that the 0.05 bias in MODIS AOD yields a cut-off of 5.1 µg/m³, where about 0.05*120 =F 6 µg/m³ is ideally expected. The close similarity gives confidence in the applicability of the determined AOD-$PM_{2.5}$ relationship.

For AATSR, only 5 retrievals were available that can be linked to ground-level $PM_{2.5}$ data. This number of data points is too low for a reliable assessment. Again, this low number indicates the low overpass frequency of AATSR compared to MODIS.

6.4 Satellite derived $PM_{2.5}$ maps

To estimate the $PM_{2.5}$ concentration field over the Netherlands, the AOD-$PM_{2.5}$ relationship was applied to the annual composite map presented in Section 6.1. A mask was applied over the data to exclude areas with large bodies of surface water, as these may be affected by large syste-

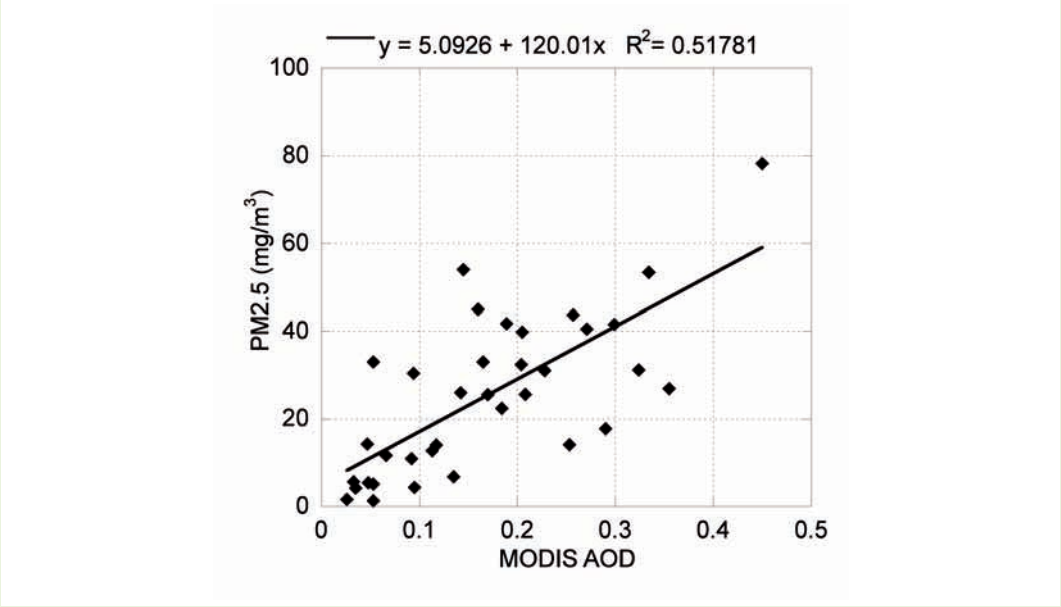

Figure 6.3 Measured $PM_{2.5}$ concentration as function of MODIS AOD.

matic errors. For this purpose, the gridded land-use database (derived from Corine) was used which is used in the LOTOS-EUROS model. All 10x10 km² grid cells with more than 10%surface water coverage were excluded from the analysis. This also excluded the North Sea. Local sea spray emissions may significantly contribute to the AOD over sea. Thus, the application area was limited to continental conditions as the influence of the marine aerosols is not accounted for in the relationship between AOD and $PM_{2.5}$ as determined at Cabauw.

The first assessment of the $PM_{2.5}$ distribution based on MODIS AOD in combination with the established AOD-$PM_{2.5}$ relationships from Cabauw is presented in Figure 6.4. The map shows estimated $PM_{2.5}$ levels, based on averaging over situations with predominantly easterly and southerly flow. Over the Netherlands, $PM_{2.5}$ levels between 22 and 30 µg/m³ are estimated for these meteorological conditions. Some features of the spatial distribution within the Netherlands do not appear to be very realistic. However, a thorough validation cannot be performed because of the lack of well-calibrated $PM_{2.5}$ measurements for this period across the Netherlands, and because of uncertainties in the emissions and modelling of $PM_{2.5}$.

Nevertheless, features such as the high $PM_{2.5}$ values near the coast of North Holland, Friesland and Groningen appear to be unrealistic. This might be caused by systematic errors in the MODIS AOD data, particularly over coastal areas and areas with inland surface water such as rivers and lakes. In such pixels, the AOD values are systematically overestimated. For that reason, pixels with more than 10% surface water were already excluded. Nevertheless, smaller inland water bodies have not been removed, and may also suffer from this overestimation of AOD. This might also explain the relatively high derived PM levels in the flow area of the large rivers. However, the AOD-$PM_{2.5}$ relationship was established within this region and no indication of overestimation of the AOD derived from MODIS was found. Lowest $PM_{2.5}$ concentrations were mapped over the Ardennes and east of the Ruhr area where levels are estimated to be around 11 µg/m³. In the Ruhr area, the resulting $PM_{2.5}$ levels are between 30 and 42 µg/m³. Strikingly, the highest $PM_{2.5}$ levels were mapped over south-west Belgium and Northern France in the vicinity of Lille.

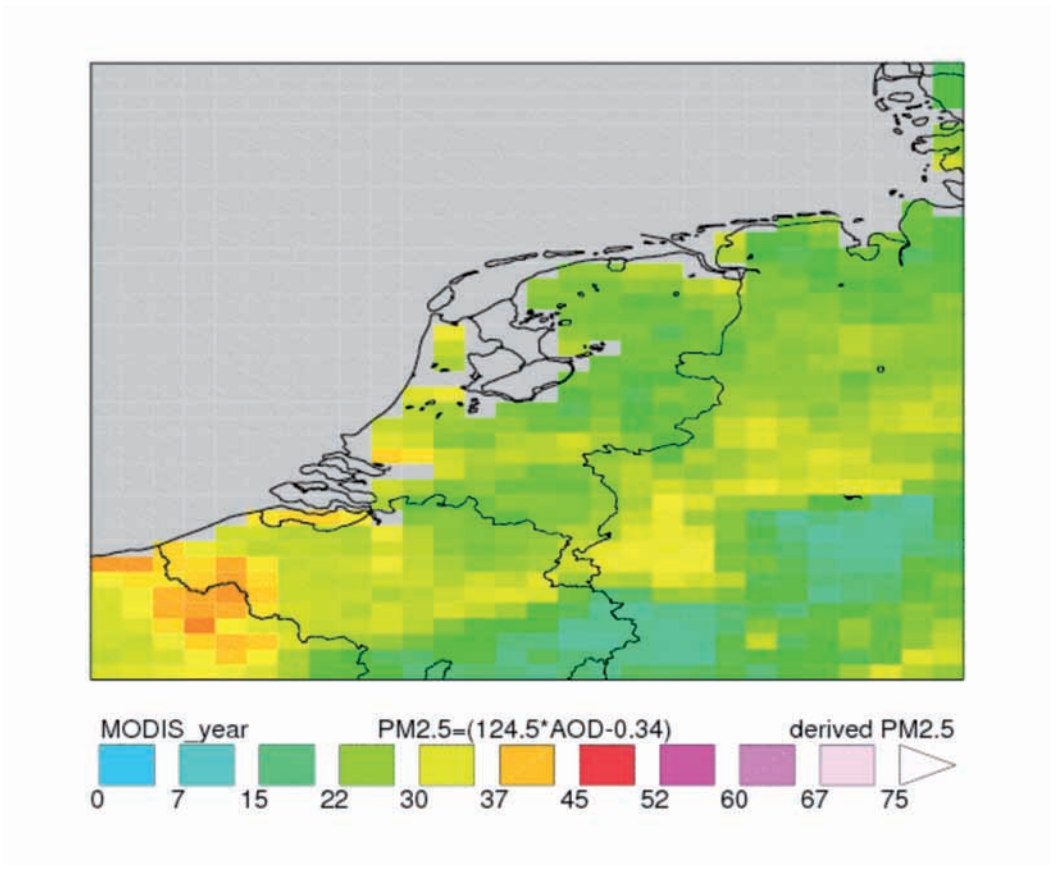

Figure 6.4 Estimated PM2.5 distribution (µg/m³) over the Netherlands and surroundings in situations of predominantly easterly and southerly flow in the period July 2006 – June 2007.

The $PM_{2.5}$-AOD relationship was derived for periods with atmospheric conditions during which satellite retrievals are available. For the Netherlands, these conditions are associated with stagnant flow or low wind speed conditions bringing polluted continental air masses to the Netherlands. The effect of the selection of days on which retrievals are available for MODIS and AERONET are presented in Table 6.2. The hours for which a MODIS retrieval is available show a mean concentration of 25 µg/m³. The hours with a lidar cloud screened AERONET observation shows a mean value of 28 µg/m³. The selection of all (V1.5) AERONET observations shows a lower mean of 23 µg/m³, reflecting the additional cases with low $PM_{2.5}$ and high AOD values which are removed by the lidar cloud screening. These averages should be compared to the mean $PM_{2.5}$ concentration of 18 µg/m³ during the SATLINK study period. In short, the average $PM_{2.5}$ based on valid AOD retrievals is not representative of a long-term average concentration, but may be higher than the annual average by typically 40 to 55 %.

Table 6.2 Comparison of the average $PM_{2.5}$ concentration (µg/m³) during the whole study period and during those hours for which AOD observations were available.

	$PM_{2.5}$	Average $PM_{2.5}$ level associated with AOD measurements		
	TEOM-FDMS	MODIS	AERONET LIDAR	AERONET all
Average	18.2	25.3	28.0	22.7
N	3946	35	226	464

6.5 Discussion

MODIS data from the new MODIS algorithm (v5.2; Levy et al., 2007) were used in this study. The new algorithm is a rigorous update of the previous version, which was used in earlier studies (e.g., PARMA). The major changes include new surface reflectivity assumptions, a new set of aerosol model optical properties derived empirically from AERONET, a new aerosol lookup table and a more elaborate inversion scheme.

This study has shown that the new collection systematically underestimates the AOD at Cabauw.. The underestimation did not show seasonal dependency, while collection 4 data used in PARMA showed a positive bias of about 50%. Thus, the new data are closer to the observed values at Cabauw. Also, the temporal correlation between MODIS and AERONET AOD increased at the Dutch stations. A preliminary evaluation by the developers also shows better agreement with AERONET (Levy et al., 2007a). However, we cannot extrapolate this finding. Thus, the data from the new collection need to be evaluated in detail for other areas in Europe.

MODIS AOD products show high AOD values above areas with suspended sediments in shallow water (Robles Gonzalez et al., 2000; Chu et al., 2002; Ichoku et al., 2005). To prevent these measurements being included in the $PM_{2.5}$ distribution, a mask was applied over the data to exclude areas with large bodies of surface water (pixels with 10% or more water coverage were excluded). As a consequence, information about coastal and water-rich areas is lost. Nevertheless, remaining artefacts caused by errors in surface albedo could still be present in the data.

The number of AOD products from satellites is increasing. Today, products are available for MODIS, MISR, AATSR, POLDER, PARASOL, OMI and others. New products are being tested for Sciamachy and SEVIRI. Each product has its own advantages and shortcomings. A worthwhile approach may be to try and combine aerosol products into one product. In this way, the strengths of single satellite products may be better exploited. For this purpose, well validated datasets need to be available. The SEVIRI data from METEOSAT could prove to be of extreme value as it provides AOD at a high temporal resolution due to its geo-stationary orbit. Hence, the amount of data and the fact that it coincides with all the other satellite products may make SEVIRI the backbone in such a composite product.

A lidar that is co-located with a sun photometer provides an opportunity to independently assess possible cloud contamination in the sun photometer data. At ground-based sites, such as Cabauw, this seems even trivial, but for satellite measurements it is not since nowadays AOD measurements from space are not coincident with lidar measurements from space. The only exception may be the use of AQUA/MODIS AOD data with CALIPSO/CALIOP lidar data. These platforms fly in a formation of satellites known as the A-train. Although this has not as yet been investigated to our knowledge, we expect that differences in footprint/swath between the sensors may be too large to use it for effective monitoring of PM2.5 from space. However, it may be useful to study the extent of cloud contamination in AOD retrievals from MODIS for those pixels for which both lidar and AOD measurements are available.

We did not have the opportunity to validate our mapping results thoroughly as no other TEOM-FDMS systems operated routinely in Dutch monitoring networks. Thus,, the estimated $PM_{2.5}$ distribution is of preliminary status and the validity and utility of our proposed mapping methodology should be further investigated. For this purpose, a number of sites with the same PM monitoring equipment, located away from the coast, should be used. The validation of $PM_{2.5}$

fields is also hampered because different atmospheric transport models show different spatial structures over the Netherlands, stemming partly from uncertainties in emissions and different treatment of atmospheric chemistry. Moreover, comparison to modelled yearly average fields is difficult as the $PM_{2.5}$ field presented here holds for conditions with southerly and easterly flows over the Netherlands and is representative for the daytime.

Nevertheless, some features of the spatial distribution within the Netherlands do not appear to be very realistic, for instance the high values of $PM_{2.5}$ near the northern coast of North Holland, Friesland and Groningen. This might be caused by systematic errors present in the MODIS AOD data, particularly over coastal areas and areas with inland surface water such as rivers and lakes. Because of the uncertainties in current satellite data of AOD, it is not expected that improved $PM_{2.5}$ maps can be constructed based on such data only in the near future. Satellite measurements of AOD will have added value, and particularly regarding the temporal variation of PM, when they are combined with atmospheric transport models and surface measurements of $PM_{2.5}$.

6.6 Cost benefit analysis

A cost-benefit analysis is presented of using satellite data for mapping $PM_{2.5}$ concentrations. Costs were determined on the basis of the costs of acquisition and processing of satellite data, operating ground-based instruments at Cabauw, and personnel costs for analysing the data. While the costs of a satellite can be high for end-users, there are no costs for the acquisition of MODIS satellite data of AOD. Costs are, therefore, determined by personnel costs to process and interpret the data.

The benefits depend on the extent to which satellite AOD data can be used to study PM. In periods with few clouds, temporal variations in AOD were shown to correlate reasonably well with temporal variations in $PM_{2.5}$ (R^2=0.6). Spatial dependent systematic errors in the AOD data, induced by the presence of mixed land/water pixels, prohibit meaningful analysis of the spatial distribution of PM using AOD data on the scale of the Netherlands. In an earlier project (PARMA), (Europe), the spatial distribution of AOD showed more realistic structures on larger scales. The reason may be that over the whole of Europe, spatial gradients in AOD are larger than within the Netherlands, while many parts of continental Europe are much less affected by the presence of mixed land/water pixels than is the case within the Netherlands.

Therefore, for monitoring temporal changes in AOD or PM, satellite data can be a cost-effective additional source of data. In a future project, AOD data will be used to improve PM forecast. It is envisaged that the satellite data provide a means to incorporate the impact of plumes with high PM loading. The satellite provides a way to incorporate into the system events that are not well incorporated in the model description, such as eastern fires, forest fires and other long range transport events.

7 Summary and conclusions

An explorative study was conducted to investigate the use of satellite observations in monitoring temporal and spatial variations in particulate matter ($PM_{2.5}$) over the Netherlands.

Analysis of the AERONET AOD data set

Since August 2006, $PM_{2.5}$ has been monitored at the atmospheric monitoring site Cabauw, which is located in a rural area in the centre of the Netherlands. In addition, other atmospheric parameters are measured simultaneously measured at Cabauw, including aerosol optical depth (AOD) and lidar backscatter profiles. This study presents the analysis of measurements at Cabauw directed at quantification of the relationship between AOD and $PM_{2.5}$ in the first year of observations. This relationship was studied using ground-based (AERONET) as well as satellite-based (MODIS and AATSR) measurements of AOD.

AERONET L1.5 showed relatively many observations of high AOD values paired to low $PM_{2.5}$ values, which suggested cloud contamination. Various methods were used to detect cloud contamination in the AERONET data in order to substantiate this hypothesis. A cloud screening method based on lidar observations was chosen to detect clouds in the AERONET L1.5 data. Application of this cloud screening method led to a rejection of about 50% of the AERONET L1.5 data because of suspected cloud contamination. Comparison with AERONET L2.0 data that became available towards the end of the project showed that almost half of the AERONET L1.5 data was not maintained in the L2.0 data set. The AERONET L2.0 data set was almost identical to the cloud-screened L1.5 data set used in this study. This gives confidence in both our cloud screening method and that used by AERONET to process L1.5 to L2.0.

The AERONET derived Ångstrøm parameter is also suitable for selecting valid AOD data because this parameter is inversely related to the cloud count of the lidar, that is, cloud presence. The use of the available lidar observations has proven to have much added value for the robustness of the analysis. The lidar method was preferred to the Ångstrøm method because the lidar provides additional insights into atmospheric conditions.

Temporal variations of AOD and $PM_{2.5}$ at Cabauw

The dependence of the relationship between AOD and $PM_{2.5}$ was studied as a function of the time of day, boundary layer height and air mass origin. The correlation between AOD and $PM_{2.5}$ increases when only data were used that had been obtained around noon, which coincides with the overpass of the satellite.

Several factors may explain the increase in the explained variability when the data are confined towards mid-day. During conditions with valid AOD retrievals, the mixing layer height during midday is generally well mixed, without residual layers. Another important factor may be related to the solar zenith angle, as a sun photometer is pointed directly at the sun. Thus, an averaging effect takes place in the observed aerosol properties and correlation with local observations decreases, particularly with large solar zenith angles. Also, cloud screening using the lidar is probably more accurate during midday as the lidar profiles the atmosphere directly above the site. Under large solar zenith angles, the observed part of the sky is rather different between sun photometer and lidar. Better similarity is obtained under small solar zenith angles.

Contra intuitively, the AOD-$PM_{2.5}$ correlation did not improve after accounting for variation in the mixing layer height. This contrasts with other studies that show a strong dependence of the AOD-PM relationship with mixing layer height and relative humidity (e.g., Gupta, 2006; Koelemeijer et al., 2006a, b). This may be due to the fact that the mixing layer did not show a strong seasonal cycle over the Cabauw site during the year, unlike many other stations in Europe that were studied in earlier work.

AOD data can only be obtained during clear sky conditions, and is biased towards conditions of stagnant flow (southerly and easterly wind directions). For such conditions, the temporal variations in AOD were shown to correlate reasonably well with temporal variations in $PM_{2.5}$ (R^2=0.6). For these conditions, and by limiting the data set to observations around noon, the following relationships were found for Cabauw: $PM_{2.5}$ =F 124.5*AOD – 0.34. The difference between the yearly average $PM_{2.5}$ data (obtained for all conditions) and $PM_{2.5}$ data for conditions with predominantly southerly and easterly flow is typically 45%.

Spatial distributions of AOD and $PM_{2.5}$ in the Netherlands

The average $PM_{2.5}$ concentration at Cabauw was 18 μg/m³. This is high in comparison with rural areas in Europe and confirms that the Netherlands is characterised by a high PM background. Satellite-derived AOD maps from AATSR and MODIS show similar mean values (0.2 to 0.25) but features observed in the spatial distributions are distinctly different. This illustrates that the interpretation of AOD maps in terms of PM is hampered because the spatially dependent systematic errors in AOD can be of the same order of magnitude as the real spatial variations in AOD across the Netherlands.

Spatial dependent systematic errors in the MODIS and AATSR AOD data, probably in part induced by the presence of mixed land/water pixels or sediments in coastal water, and lack of knowledge about the real $PM_{2.5}$ distribution prohibit a meaningful analysis of the spatial distribution of $PM_{2.5}$ using AOD data at the scale of the Netherlands. In an earlier project (PARMA), it was shown that at larger scales (Europe), the spatial distribution of AOD shows more realistic structures. The reason may be that over the whole of Europe, spatial gradients in AOD are larger than within the Netherlands, while many parts of continental Europe are much less affected by the presence of mixed land/water pixels than is the case within the Netherlands.

Because of the uncertainties in current satellite data of AOD, it is not expected that improved $PM_{2.5}$ maps for the Netherlands can be constructed based on satellite data only. Satellite measurements of AOD can have added-value, particularly regarding temporal variation in PM, when combined with atmospheric transport models and surface measurements of $PM_{2.5}$.

Acknowledgements

We would like to thank Dr. W. Knap and Dr. H. Klein Baltink (KNMI) for providing the ACPADA data and mixing layer height data, respectively. R. Otjes (ECN) is acknowledged for supplying MARGA data. We are indebted to the MODIS research community for providing satellite data.

References

Al-Saadi, J., Szykman, J., Pierce, R.B., Kittaka, C., Neil, D., Chu, D.A., Remer, L., Gumley, L., Prins, E., Weinstock, L., MacDonald, C., Wayland, R., Dimmick, F., Fishman, J., 2005. Improving national air quality forecasts with satellite aerosol observations, Bulletin of the American Meteorological Society, 86 (9), 1249-1261.

Brunekreef, B., Holgate, S.T. ,2002. Air pollution and health, The Lancet, 360, 1233-1242.

Builtjes, P.J.H., ten Brink, H.M., de Leeuw, G., van Loon, M., Robles Gonzales, C., Schaap, M., 2001. Aerosol air quality satellite data, BCRS USP-2 report 00-33, BCRS, Delft, The Netherlands.

Bureau Veritas, 2006. UK Equivalence Programme for Monitoring of Particulate Matter, report number BV/AQ/AD202209/DH/2396.

Collins, W.D., Rasch, P.J., Eaton, B.E., Khattatov, B.V., Lamarque, J-F., Zender, C.S., 2001. Simulating aerosols using a chemical transport model with assimilation of satellite aerosol retrievals: Methodology for indoex, J. Geophys. Res., 106, 7313-7336

Chu, D.A., Kaufman, Y.J., Ichoku, C., Remer, L.A, Tanré, D., Holben, B.N., 2002. Validation of MODIS aerosol optical thickness retrieval over land, Geophys. Res. Lett., 29, NO. 12, doi:10.1029/2001GL013205.

Chu, D.A., Kaufman, Y.J., Zibordi, G., Chern, J.D., Mao, J., Li, C., Holben, B.N., 2003. Global monitoring of air pollution over land from the Earth Observing System-Terra Moderate Resolution Imaging Spectroradiometer (MODIS), J. Geophys. Res., 108, 4661, doi:10.1029/2002JD003179.

De Haan J.F., P.B. Bosma and J.W. Hovenier, 1987. The adding method for multiple scattering calculations of polarised light, Astron. Astrophys., 183, 371-391.

De Haij, M., W. Wauben and H. Klein Baltink, 2007. Continuous mixing layer height determination using the LD-40 ceilometer: a feasibility study, KNMI, De Bilt.

De Meij, A., S. Wagner, N. Gobron, P. Thunis, C. Cuvelier, F. Dentener, M. Schaap, 2007. Scale issues in aerosol modeling: a case study on chemical and optical properties over the greater Milan area (Italy), June 2001, Atmospheric Research, 85, 243–267.

Dockery D.W., Pope III, C.A., Xu, X., Spengler, J.D., Ware, J. H., Fay, M.E., Ferris, B.G. and Speizer, F.E., 1993. An Association between Air Pollution and Mortality in Six U.S. Cities, The New England Journal of Medicine, 329, 1753-1759.

Dubovik, O. and King, M. D., 2000. A flexible inversion algorithm for retrieval of aerosol optical properties from Sun and sky radiance measurements, J. Geophys. Res., 105, 20 673–20 696.

Dubovik, O., Smirnov, A., Holben, B. N., King, M. D., Kaufman, Y. J., Eck, T. F., and Slutsker, I, 2000. Accuracy assessments of aerosol optical properties retrieved from AERONET sun and sky-radiance measurements, J. Geophys. Res, 105, 9791–9806.

Dubovik, O., Lapyonok, T., Kaufman, Y.J., Chin, M., Ginoux, P., Remer, L., Holben, B.N., 2004. Retrieving sources of fine aerosols from MODIS and AERONET observations by inverting GOCART model, Proceedings of SPIE - The International Society for Optical Engineering, 5652, pp. 66-75.

Dürr, B., Philipona, R., 2004. Automatic cloud amount detection by surface longwave downward radiation measurements. Journal of Geophysical Research D: Atmospheres, 109 (5), D05201 1-9.

Eck, T. F., Holben, B. N., Reid, J. S., Dubovik, O., Smirnov, A., O'Neill, N. T. Slutsker, I., and Kinne, S., 1999. Wavelength dependence of the optical depth of biomass burning, urban, and desert dust aerosol, J. Geophys. Res., 104, 31 333–31 350.

EEA, 2007. Europe's environment - The fourth assessment. EEA, Copenhagen.

Engel-Cox, J.A., Holloman, C.H., Coutant, B.W. and Hoff, R.M., 2004., Qualitative and quantitative evaluation of MODIS satellite sensor data for regional and urban scale air quality, Atmos. Environ, 38, 2495-2509

Engel-Cox, J. A., Hoff, R. M., Rogers, R., Dimmick, F., Rush, A. C., Szykman, J. J., Al-Saadi, J., Chu, D. A., Zell, E. R., 2006. Integrating lidar and satellite optical depth with ambient monitoring for 3-D dimensional particulate characterisation. Atmospheric Environment 40, 8056-8067.

Gupta, P., Christopher, S.A., Wang J., Gehrig, R., Lee. Y., Kumar, N., 2006. Satellite remote sensing of particulate matter and air quality assessment over global cities, Atmospheric Environment 40 (2006) 5880–5892.

Gupta, P., Christopher, S.A., Box, M.A., Box, G.P., 2007. Multi year satellite remote sensing of particulate matter air quality over Sydney, Australia. International Journal of Remote Sensing, 28(20), 4483-4498.

Gupta, P. and Christopher, S.A., 2008. Seven year particulate matter air quality assessment from surface and satellite measurements, Atmos. Chem. Phys. Discuss., 8, 327-365

Holben B. N., Eck, T.F., Slutsker, I., Tanre, D., Buis, J.P. Setzer, A., Vermote, E., Reagan, J.A., Kaufman, Y.F., Nakajima, T., Lavenu, F., Jankowiak, I., Smirnov, A., 1998. AERONET-A Federated Instrument Network and Data Archive for Aerosol Characterisation, Rem. Sens. of the Env., 66, 1-16.

Holben, B. N., Tanre, D., Smirnov, A. et al., 2001. An emerging ground-based aerosol climatology: Aerosol optical depth from AERONET, J. Geophys. Res., 106, 12 067–12 097.

Hutchison, K.D., 2003. Applications of MODIS satellite data and products for monitoring air quality in the state of Texas, Atmos. Environ., 37, 2403-2412.

Ichoku, C., Remer, L.A., and Eck, T.F., 2005. Quantitative evaluation and intercomparison of morning and afternoon Moderate Resolution Imaging Spectroradiometer (MODIS) aerosol measurements from Terra and Aqua, J. Geophys. Res., 110, D10S03, doi:10.1029/2004JD004987.

Ichoku, C., Chu, D.A., Mattoo, A., Kaufman, Y. J., Remer, L.A, Tanre, D., Slutsker, I., Holben, B.N., 2002. A spatio-temporal approach for global validation and analysis of MODIS aerosol products, Geophys. Res. Let., 29, DOI: 10.1029/2001GL013206.

Kacenelenbogen, M., Léon, J.-F., Chiapello, I., Tanré, D., 2006. Characterisation of aerosol pollution events in France using ground-based and POLDER-2 satellite data. Atmospheric Chemistry and Physics 6, 4843-4849.

Kaufman, Y.J. and Tanré, D., 1998. Algorithm for Remote Sensing of Tropospheric Aerosol from MODIS, Product ID MOD04.

Klett, J. D., 1985. Lidar inversion with variable backscatter/extinction ratios, Applied Optics, 24, 1638 - 1643.

Koelemeijer R. B. A., Stammes P., Hovenier J. W., and De Haan J. D., 2001. A fast method for retrieval of cloud parameters using oxygen A-band measurements from the Global Ozone Monitoring Instrument, J. Geophys. Res., 106, 3475-3490.

Koelemeijer, R.B.A., Schaap, M., Timmermans, R.M.A., Homan, C.D., Matthijsen, J., van de Kassteele, J., Builtjes, P.J.H., 2006a. Mapping aerosol concentrations and optical thickness over Europe – PARMA final report, MNP report 555034001, Bilthoven, the Netherlands.

Koelemeijer, R.B.A., Homan, C.D., and Matthijsen, J., 2006b. Comparison of spatial and temporal variations of aerosol optical thickness and particulate matter in Europe, Atmos. Environ., 40, 5304-5315.

Kokhanovsky A., and the Aerosol Retrieval Team, 2007. The determination of aerosol optical thickness over Germany using different satellite algorithms and instruments: an inter-comparison study based on spectral top-of-atmosphere measurements of AATSR, MERIS, MISR, MODIS, POLDER, and SCIAMACHY, Geophysical Research Abstracts, Vol. 9, 01222.

Koren, I., Kaufman, Y.J., Rosenfeld, D., Remer, L.A., Rudich, Y., 2005. Aerosol invigoration and restructuring of Atlantic convective clouds, Geophysical Research Letters, 32 (14), pp. 1-4.

Levy, R.C., Remer, L.A., Mattoo, S., Vermote, E.F., Kaufman, Y.J., 2007. Second-generation operational algorithm: Retrieval of aerosol properties over land from inversion of Moderate Resolution Imaging Spectroradiometer spectral reflectance, Journal of Geophysical Research D: Atmospheres 112 (13), art. no. D13211.

Levy, R.C., Remer, L.A., Dubovik, O., 2007a. Global aerosol optical properties and application to Moderate Resolution Imaging Spectroradiometer aerosol retrieval over land, Journal of Geophysical Research D: Atmospheres, 112 (13), art. no. D13210.

Levy, R.C., Remer, L.A., Mattoo, S., Vermote, E.F., Kaufman, Y.J., 2007b. Second-generation operational algorithm: Retrieval of aerosol properties over land from inversion of Moderate Resolution Imaging Spectroradiometer spectral reflectance, Journal of Geophysical Research D: Atmospheres, 112 (13), art. no. D13211.

Liu, L., A.A. Lacis, B.E. Carlson, M.I. Mishchenko, and B. Cairns, 2005. Improving GCM Aerosol Climatology using Satellite and Ground-Based Measurements, 15th ARM Science Team Meeting Proceedings, Daytona Beach, Florida, March 14-18, 2005.

Liu, Y., Sarnat, J. A., Kilaru, V., Jacob, D. J., Koutrakis, P., 2005. Estimating ground-level $PM_{2.5}$ in the Eastern United States using satellite remote sensing. Environmental Science and Technology 39, 3269-3278.

Pal, S. R., et al., 1992. Automated method for lidar determination of cloud-base height and vertical extent, Applied Optics, 31, 1488 - 1494.

Pope III, C.A., Dockery, D.W., Schwartz, J., 1995. Review of epidemiological evidence of health effects of particulate air pollution, Inhalation Toxicology, 7, 1–18.

Pelletier, B., Santer, R., Vidot, J., 2007. Retrieving of particulate matter from optical measurements: A semiparametric approach, Journal of Geophysical Research D: Atmospheres, 112 (6), art. no. D06208.

Putaud, J., Raesa, F., Van Dingenen, R., Bruggemann, E., Facchini, M., Decesari, S., Fuzzi, S., Gehrig, R., Hueglin, C., Laj, P., Lorbeer, G., Maenhaut, W., Mihalopoulos, N., Mueller,K., Querol, X., Rodriguez, S., Schneider, J., Spindler, G., ten Brink, H., Torseth, K, Wiedensohler, A., 2004. A European aerosol phenomenology - 2:chemical characteristics of particulate matter at kerbside, urban, rural and background sites in Europe, Atmospheric Environment, 38, 2579–2595.

Remer, L.A., Kaufman, Y.J., Tanré, D., Mattoo, S., Chu, D.A., Martins, J.V., Li, R.-R., Ichoku, C. , Levy, R.C., Kleidman, R.G., Eck, T.F., Vermote, E. and Holben, B.N., 2005. The MODIS Aerosol Algorithm, Products, and Validation, J. Atmos. Sci., 62, 947-973.

Robles Gonzalez, C., Veefkind, J. P., and de Leeuw, G., 2000. Aerosol optical depth over Europe in August 1997 derived from ATSR-2 data, Geophysical Research Letters, 27 (7), 955–958.

Robles-Gonzalez, C., 2003. Retrieval of aerosol properties using ATSR-2 observations and their interpretation, PhD-thesis, Utrecht University, Utrecht, the Netherlands.

Schaap, M., Muller, K., and ten Brink, H. M., 2002. Constructing the European aerosol nitrate concentration field from quality analysed data, Atmos. Environ, 36, 8, 1323–1335.

Schaap, M., Timmermans, R.M.A, Koelemeijer, R.B.A, de Leeuw, G., Builtjes, P.J.H., 2008. Evaluation of MODIS aerosol optical thickness over Europe using sun photometer observations, Atmos. Environ., 42, 2187–2197, doi:10.1016/j.atmosenv.2007.11.044.

Cambridge Research Laboratory, Hanscom Air Force Base, MA, 10 pp, 1979.

Smirnov, A., Holben, B. N.,Eck, T. F., Dubovik, O., and Slutsker, I., 2000. Cloud screening and quality control algorithms for the AERONET data base, Remote Sens. Environ., 73(3), 337–349.

Stammes P., 1994. Errors in UV reflectivity and albedo calculations due to neglecting polarisation, in: SPIE Proc. Vol. 2311, pp. 227-235.

Stammes, P. and J.S. Henzing, 2000. Multispectral aerosol optical thickness at De Bilt, 1997-1999. J. Aerosol Sci., 31, 283–284.

van de Kassteele, J., Koelemeijer, R.B.A., Dekkers, A.L.M., Schaap, M., Homan, C.D., Stein, A., 2006., Statistical mapping of PM_{10} concentrations over Western Europe using secondary information from dispersion modeling and MODIS satellite observations, Stoch Environ Res Risk Assess, DOI 10.1007/s00477-006-0055-4.

van Donkelaar, A., Martin, R. V., and Park, R. J., 2006. Estimating ground-level $PM_{2.5}$ using aerosol optical thickness determined from satellite remote sensing, J. Geophys. Res., 111, D21201, doi:10.1029/2005JD006996.

Veefkind, J. P., de Leeuw, G., and Durkee, P. A., 1998. Retrieval of Aerosol Optical Depth over Land using two angle view Satellite Radiometry during TARFOX, Geophysical Research Letters, 25, 3135–3138.

Veefkind, J. P., de Leeuw, G., Stammes, P., and Koelemeijer, R. B. A., 2000. Regional Distribution of Aerosol over land derived from ATSR-2 and GOME, Rem. Sens. of the Env., 74, 377–386.

Volz, F.E., 1972. Infrared refractive index of atmospheric aerosol substances, Applied Optics, 11 (4), 755-759.

Wang J. and Christopher, S.A., 2003. Intercomparison between satellite-derived aerosol optical thickness and $PM_{2.5}$ mass: implications for air quality studies, Geophys. Res. Lett., 30 (21), 2095, doi:10.1029/2003GL018174.

Wen, G., Marshak, A., Cahalan, R.F., Remer, L.A., Kleidman, R.G., 2007. 3-D aerosol-cloud radiative interaction observed in collocated MODIS and ASTER images of cumulus cloud fields, Journal of Geophysical Research D: Atmospheres, 112 (13), art. no. D13204.

WHO, 2006. Health risks of particulate matter from long-range transboundary air pollution European Centre for Environment and Health - Bonn Office, Joint WHO / Convention Task Force on the Health Aspects of Air Pollution. WHO Regional Office for Europe, Copenhagen.

Yu, H., Kaufman, Y.J., Chin, M., Feingold, G., Remer, L.A., Anderson, T.L., Balkanski, Y., Bellouin, N., Boucher, O., Christopher, S., DeCola, P., Kahn, R., Koch, D., Loeb, N., Reddy, M.S., Schulz, M., Takemura, T., Zhou, M., 2006. A review of measurement-based assessments of the aerosol direct radiative effect and forcing. Atmospheric Chemistry and Physics, 6 (3), pp. 613-666.

Appendix A: Outreach

The results of this project have been presented at various scientific workshops and conferences. Furthermore, a website has been constructed on which the results of the SATLINK project, together with the earlier NIVR- project of this consortium (PARMA and HIRAM) are accessible to the general public: www.rivm.nl/milieuportaal/onderwerpen/lucht.
Also, a scientific paper has been submitted to a peer-reviewed journal.

Presentations

- Apituley, A., M. Schaap, R. Koelemeijer, R. Timmermans, R. Schoemaker, G. de Leeuw, Construction of satellite derived PM2.5 maps using the relationship between AOD and PM2.5 at the Cabauw Experimental Site for Atmospheric Research (CESAR) – The Netherlands, oral presentation at IGARSS 2008, July 2008, Boston, Massachusetts.
- Builtjes, P., M. Schaap, C. Bremmer et al., On the use of remote sensing data for air quality monitoring, colloquium for the monitoring group DGM of VROM, September 19th 2007, The Hague, the Netherlands.
- Koelemeijer, R. Atmospheric composition from space: its role in environmental assessment, TROPOMI workshop, KNMI, 5-6 March 2008, De Bilt.
- Schaap, M., A. Apituley, A. Segers, H. Klein Baltink, R. Timmermans, R. Koelemeijer, D. Swart, G. de Leeuw, On the relation between AOD and $PM_{2.5}$ at the research station of Cabauw (NL), oral presentation at the European Aerosol Conference, 9-14 September, Salzburg, Austria.
- Schaap, M., R. Timmermans, R. Koelemeijer, and P. Builtjes, Assimilation of MODIS AOD in a regional chemistry transport model, oral presentation at A-train symposium, Lille, 22-25 October 2007.
- Schaap, M., Apituley, A., Koelemeijer, R.B.A., Timmermans, R.M.A, de Leeuw, G., Mapping the $PM_{2.5}$ Distribution in the Netherlands Using MODIS AOD, oral presentation at the AGU joint assembly, 27-30 May 2008, Fort Lauderdale, USA.

Publications

Schaap, M., Apituley, A., Koelemeijer, R.B.A., Timmermans, R.M.A, de Leeuw, G. (2008), Exploring the relation between aerosol optical depth and $PM_{2.5}$ at Cabauw, the Netherlands, paper in preparation for submission to Atmospheric Environment

Schaap, M., Timmermans, R.M.A, Koelemeijer, R.B.A, de Leeuw, G., Builtjes, P.J.H. (2008), Evaluation of MODIS aerosol optical thickness over Europe using sun photometer observations, Atmos. Environ., 42, 2187–2197, doi:10.1016/j.atmosenv.2007.11.044 (Based on both NIVR-GO PARMA and SATLINK)

Appendix B: Effect of cloud screening for Spring 2007

The influence of the different cloud screening methods for Spring 2007 is presented. See also Chapter 4.

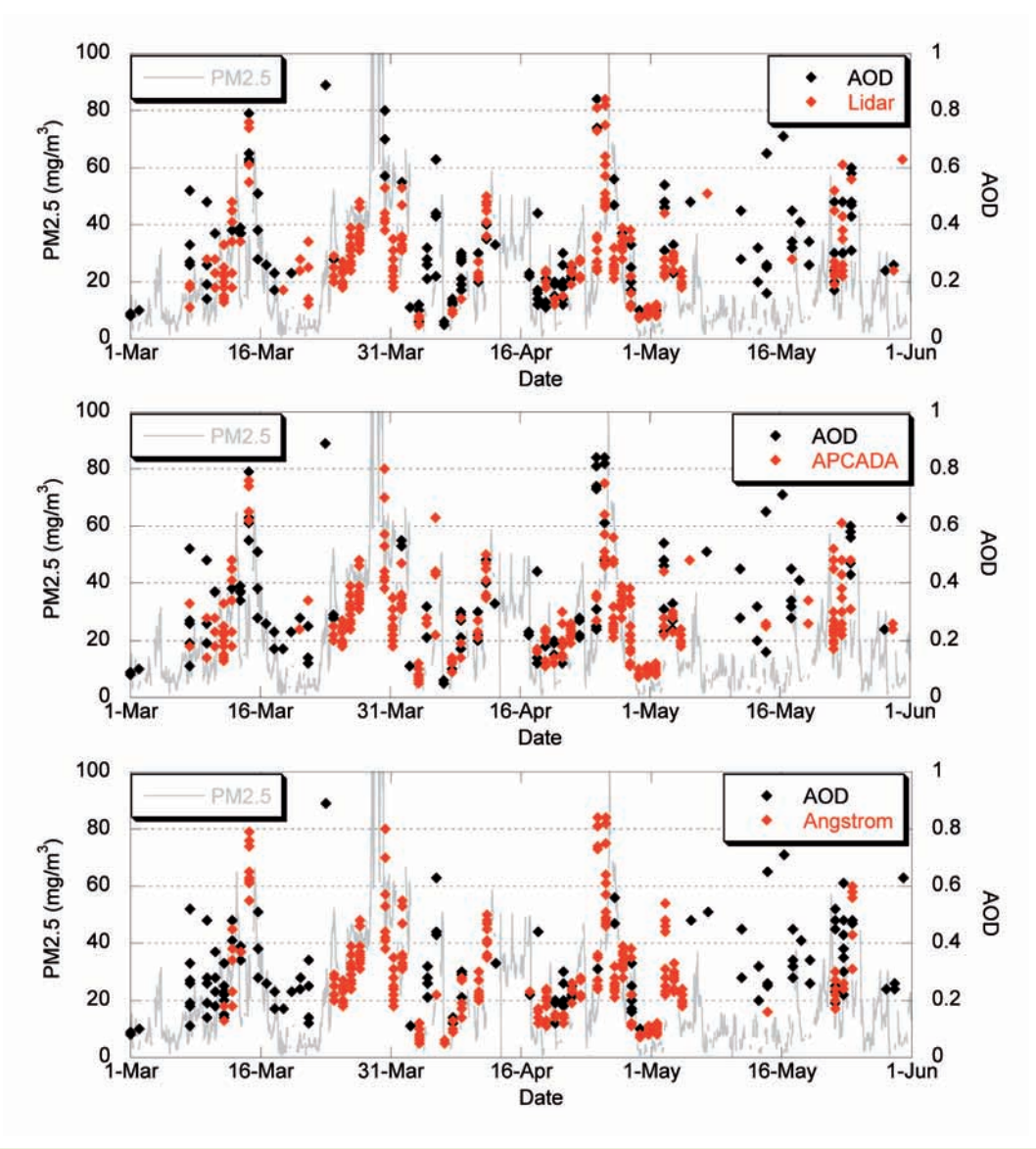

Figure B1 Time series of $PM_{2.5}$ and AOD data regarded to be cloud free (red) or suspected of cloud contamination (black) for the methodology based on the LIDAR (upper panel), APCADA (middle panel) and the Ångstrøm parameter (lower panel) for spring 2007.

Appendix C: National User Support Programme 2001-2005

The National User Support Programme 2001-2005 (NUSP) is being carried out by the Netherlands Agency for Aerospace Programmes (NIVR) and the SRON Netherlands Institute for Space Research. NUSP is financed from the national space budget. The NUSP subsidy arrangement contributes to the development of new applications and policy-supporting research, institutional use and use by private companies.
NUSP aims to::

- Support those in the Netherlands, who are users of information from existing and future European and non-European earth observation systems in the development of new applications for scientific research, industrial and policy research and operational use;
- Stimulate the national and international service market based on space-based derived operational geo-information products by means of strengthening the position of the Dutch private service sector;
- Assist in the development of a national geo-spatial data and information infrastructure, in association with European and non-European infrastructures, based on Dutch user needs;
- To supply information to the general public on national and international space-based geo-information applications, new developments and scientific research results.

More information about the National User Support Programme 2001-2005 can be found at http://www.ao-go.nivr.nl

The use of satellite measurements as a proxy for $PM_{2.5}$

This study explores the use of satellite observations of Aerosol Optical Depth (AOD) in monitoring temporal and spatial variations in particulate matter ($PM_{2.5}$) in the Netherlands. AOD data can only be obtained under clear sky conditions, and are biased towards conditions of stagnant flow (southerly and easterly wind). Under such conditions, the AOD correlates reasonably well with $PM_{2.5}$ (R^2=0.6), suggesting that temporal variations in AOD can be used as a proxy for temporal variations in $PM_{2.5}$.

The average $PM_{2.5}$ concentration at Cabauw, a central site for atmospheric research in the Netherlands, was 18 µg/m^3. This confirms the relatively high background $PM_{2.5}$ in the Netherlands compared to rural areas in Europe. Satellite derived AOD maps from AATSR and MODIS show similar mean values, but observed features in the spatial distributions are distinctly different. This illustrates that interpretation of these AOD maps in terms of PM is hampered because of spatially dependent systematic errors in AOD which are of the same order of magnitude as spatial variations in AOD across the Netherlands.

Because of the uncertainties in current satellite data of AOD, it is not expected that better $PM_{2.5}$ maps for the Netherlands can be constructed based on these satellite data only. Satellite measurements of AOD have added-value, however, particularly with regard to temporal variation in PM, when combined with atmospheric transport models and surface measurements of $PM_{2.5}$.

A publication of the
Netherlands Environmental Assessment Agency
P.O. Box 303, 3720 AH Bilthoven, The Netherlands
www.pbl.nl/en